



16th International Benchmark Workshop on Numerical Analysis of Dams

Proceedings

Mateja Klun
Andrej Kryžanowski
Nina Humar

Ljubljana, 5th - 6th April, 2022

16TH INTERNATIONAL BENCHMARK WORKSHOP ON NUMERICAL
ANALYSIS OF DAMS- PROCEEDINGS
16. MEDNARODNA KONFERENCA O NUMERČNI ANALIZI PREGRAD- ZBORNİK PRISPEVKOV

Editors/uredniki:

Mateja Klun, Andrej Kryžanowski, Nina Humar

Publishers/izdajatelji:

Slovenian National Committee on Large Dams- SLOCOLD

Slovenski nacionalni komite za velike pregrade – SLOCOLD

UNESCO Chair on Water-related Disaster Risk Reduction, University of Ljubljana

UNESCO katedra za zmanjševanje tveganj ob vodnih ujmah, Univerza v Ljubljani

© SLOCOLD 2022

Ljubljana, 2024

Kataložni zapis o publikaciji (CIP) pripravili v Narodni in univerzitetni knjižnici v Ljubljani

COBISS.SI-ID 190152451

ISBN 978-961-94027-1-9 (Slovenski nacionalni komite za velike pregrade – SLOCOLD, PDF)

The editors acknowledge the contribution by many of our colleagues who contributed to the successful realization of the event and wish to express their deep gratitude to them.

The Editors also gratefully thank:

The team of Formulators for the tremendous work done to define the theme content and for providing the synthesis of the results obtained by all the contributors and participants,

Slovenian national committee on large dams, SLOCOLD and Faculty of Civil and Geodetic Engineering of Ljubljana for the organizational support,

the sponsors who provided financial support and facilities for the workshop.

Promoted by the ICOLD Technical Committee Computational Aspects of Analysis and Design of Dams and organized by Slovenian national committee on large dams SLOCOLD and Faculty of Civil and Geodetic Engineering of Ljubljana.



ICOLD Technical Committee A
Computational Aspects of
Analysis and Design of Dams



The proceedings are issued under the auspices of UNESCO chair on water – related disaster risk reduction.

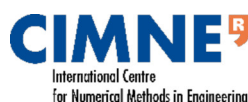
Univerza v Ljubljani



UNESCO katedra za zmanjševanje
tveganj ob vodnih ujmah
Univerza v Ljubljani



Sponsors and supporters:



Mateja Klun, Faculty of civil and geodetic engineering of Ljubljana
Andrej Kryžanowski, Faculty of civil and geodetic engineering of Ljubljana
Nina Humar, Slovenian national committee on large dam

BEHAVIOR PREDICTION OF A CONCRETE ARCH DAM

Stevcho Mitovski

Faculty of Civil Engineering, Ss. Cyril and Methodius University in Skopje, Skopje, North Macedonia

Gjorgji Kokalanov

Faculty of Civil Engineering, Ss. Cyril and Methodius University in Skopje, Skopje, North Macedonia

Ljupcho Petkovski

Faculty of Civil Engineering, Ss. Cyril and Methodius University in Skopje, Skopje, North Macedonia

Frosina Panovska

Faculty of Civil Engineering, Ss. Cyril and Methodius University in Skopje, Skopje, North Macedonia

Vasko Kokalanov

Faculty of Computer Science, Goce Delchev University, Stip, North Macedonia

ABSTRACT: The assessment of the structural stability and the behavior of the dam during construction and service period is of vital importance. In the paper are presented acknowledgments from the numerical analysis of concrete arch dam under static and hydraulic (seepage) action, by application of Finite Element models (code SOFiSTiK) and Neural Networks models (NeuralTools code). The aim of the task is to predict the dam behavior, that includes calibration (based on monitoring data) and prognosis stage (short-term and long-term) focusing on variables such as radial displacements, crack displacements, piezometric levels and seepage. Coupled thermo-mechanical analysis and seepage analysis in time domain were carried out the for calibration and prognosis stage of the specified variables, in case of FEM modelling. The conclusion from the both numerical experiments (FEM and Neural Networks) is that the dam behavior, with adopted geometry and material, is within the expected mode.

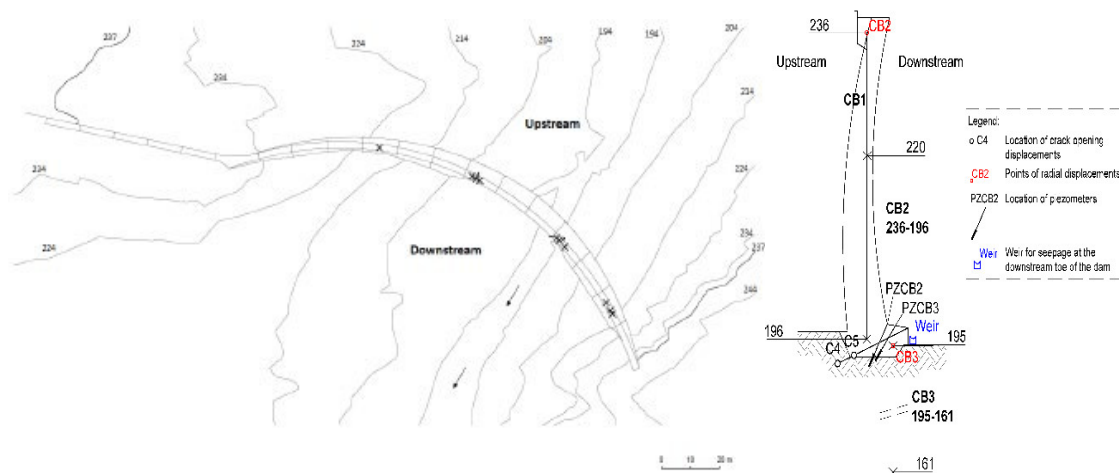
1 INTRODUCTION

The dams, having in consideration their importance, dimensions, complexity of the problems that should be solved during the process of designing and construction along with the environmental impact are lined up in the most complex engineering structures (Tanchev, 2014; Novak & all., 2007). The assessment of the structural stability and the behavior of the dam during construction, at full reservoir and during the service period is of paramount importance for such structures.

Static stability of concrete dams is confirmed with analysis (research) of the response of the structure (dam) under action of static loads (Mitovski & all, 2015, Mitovski & all, 2017a, Mitovski & all, 2017b]. In this paper are systemized acknowledgments from the linear and nonlinear static numerical analysis of concrete arch dam, obtained with application of Finite Element Method models (code SOFiSTiK) and Neural Networks models. Namely, here below will be illustrated output data from the numerical experiment for prediction behavior of the arch dam Dam EDF, located in France. The aim of the task is to predict the dam behavior, that includes calibration (based on monitoring data) and prognosis stage (short-term and long-term) focusing on variable such as radial displacements (two pendulums in central block of the dam), crack displacements (sensor at the rock-concrete interface), piezometric levels (vibrating wire piezometers at the rock-concrete interface) and seepage (weir at the downstream of the dam).

2 CASE STUDY

The analyzed dam is located in southern France, constructed in period 1957-1960. It is a case of double curvature arch dam, with asymmetric shape due to the valley formation (Fig. 1). The dam foundation is laminated metamorphic slate with high compressive strength, with present anisotropy in the left bank. The dam height above the foundation is $H=45$ m, with crest thickness of 2 m and base thickness of 6 m.



evaluate its stability. The program SOFiSTiK in its library contains and various standards and constitutive laws (linear and non-linear) for structures analysis.

The numerical experiment includes following steps, typical for this type of analysis: (1) choice of material properties and constitutive laws (concrete and rock); (2) discretization of the dam and the rock foundation and (3) simulation of the dam behavior for the typical loading states (as required in the topic formulation).

3.1.1 Material properties

The linear material properties for the dam body (concrete) and the foundation (rock) are systematized in Table 1. The specified parameters are adopted according to Theme A formulation (Malm & all, 2021) as well and previous carried out analysis and reference literature (Desai & Gallagher, 1984, SOFiSTiK, 2022, EC 2, 1992, Mitovski, 2015, USBR, 1977).

Table 1. Material parameters.

Zone		dam body (concrete)	rock	Comment
γ_{spec}	kN/m ³	24.0	27.0	Unit weight
k_s	m/s		2.0e-05	Permeability coefficient
ν		0.350	0.450	Poisson coefficient
Alpha	1/C°	7.0E-06		Thermal expansion coefficient
E	GPa	22	3	Young's modulus of elasticity

Additionally, for carrying out of non-linear analysis of the dam in order to calibrate and predict the relative distance values at interface dam-foundation is applied non-linear constitutive law for concrete based on elasto-plastic material law Lade with non-associated flow rule from SOFiSTiK library of materials (Table 2).

Table 2. Non-linear material parameters for concrete.

Zone		dam body (concrete)	Comment
γ_{spec}	kN/m ³	24.0	Unit weight
ν		0.350	Poisson coefficient
Alpha	1/C°	7.0e-06	Thermal expansion coefficient
E	GPa	22	Young's modulus of elasticity
P3	kN/m ²	2900	Uniaxial tensile strength
m		1	Parameter for curvature of the yield surface towards the hydrostatic axis
η		88162	Yield function
f_{cd}	kN/m ²	33333	Compressive strength
ϵ_{tu}	‰	0.2	Tensile failure strength

3.1.2 Discretization of dam body and foundation by finite elements

Numerical analysis of the arch dam is carried out by spatial (3D) model, where the dam body and the foundation are modeled with volume elements, by full reproduction of the finite element model formulation data. A powerful and reliable finite element should be applied in case where an analysis of structure with complex geometry and behavior is required, having in consideration that the correctly calculated deformations and stresses are of primary significance for assessment of the dam stability. In this case, for discretization of the dam body and the rock foundation are applied finite element type brick, by 4 nodes, identical to C3D4 element from ABAQUS and kinematic constraints at the interface dam-rock foundation. Namely, the model is composed of dam body and rock foundation with constraints at the interface dam-foundation.

The spatial (3D) model has geometrical boundaries, limited to horizontal and vertical plane. In these planes are defined the boundary condition of the model (Figure 2). The curvature plane in the lowest zone of the model is adopted as non-deformable boundary condition (fixed displacements in XYZ direction), vertical planes perpendicular on X-axis are boundary condition

by applying fixed (zero) displacements in X-direction and vertical planes perpendicular on Y-axis are boundary condition by applying fixed (zero) displacements in Y-direction. The discretization is conveyed by including zones of various materials in the model – concrete and rock foundation. The dam is modeled as monolithic structure.

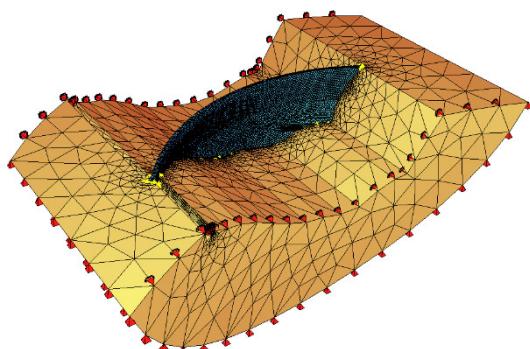


Figure 2: View of the numerical model, discretized with total of 186583 elements and 39419 nodes.

3.1.3 Dam loading scenarios for calibration and prognosis stage

The dam loading is directly correlated with the calibration and prognosis stage for the dam behavior. The numerical analysis is carried out by coupled thermo-mechanical model and hydraulic (seepage) model for analysis of the dam behavior in the calibration and prediction stage. The thermal effect of the dam is simulated by applying temperature loading of the dam body according to air temperature time series as uniform distribution within the volume (brick) elements. The assumption is that the temperature loading in the dam body is uniformly distributed in the various time steps and approximately in range of the air temperature. The temperature effect is coupled with the hydrostatic loading in accordance with the specified water levels from the reservoir for the identical time steps. The hydrostatic loading is applied at upstream face of the dam as spatial load in accordance with the water levels in the reservoir. The calibration process is carried out by combined choice of extreme (highest) values for the air temperature T_a , water levels in the reservoir WL and measured values for the variables records within the monitoring process. The method of adoption of the extreme values per dates for time series of pendulums CB2 means that are chosen maximal and minimal values from the recorded data. Namely, in such a way, by analogy are adopted records for the water levels and temperature, thus obtaining a representative number of load cases in order to assess the dam behavior, that are being run within the model.

Identical approach is applied and for the prognosis stage. Namely, for the short-term prognosis is carried out calculation of the dam response for all time steps from January-June, 2013 (total of 184), while for the long-term prognosis is applied also combined choice of extreme values for period July, 2013-December, 2017, regarding the water levels in the reservoir and temperature T_a , thus obtaining total a representative number of load cases for the various variables with aim to predict the dam's behavior, that are being run within the model. Static loading scenarios includes self-weight of the concrete arch dam and the rock foundation.

3.2 Neural networks modelling of the dam

Artificial neural networks are typical example of a modern interdisciplinary subject that helps solving various different engineering problems which could not be solved by the traditional modelling and statistical methods (I. Flood K. N., 1994). Neural networks are capable of collecting, memorizing, analyzing and processing large number of data gained from some experiments or numerical analyses. They are an illustration of sophisticated modelling technique that can be used for solving many complex problems. The trained neural network serves as an analytical tool for qualified prognoses of the results, for any input data which were not included in the learning process of the network. Their operation is reasonably simple and easy, yet correct and precise. The artificial neural networks, together with the fuzzy logic and genetic algorithms, belong to the group of symbolic methods of intelligent calculations and data processing that operate according to the principles of soft computing. Neural networks are developed as a result of the positive

features of a few different research directions: data processing, neuro-biology and physics (I. Flood K. N., 1994). Researches around the world showed that neural networks have an excellent success in prediction of data series and that is why they can be used for creating prognostic models that could solve different problems and tasks (I. Flood K. N., 1994; I. Flood C. P., 1996). For practical application of artificial neural networks, it is not necessary to use complex neuron models. Therefore, the developed models for artificial neurons only remind us to the structure of the biological ones and they have no pretension to copy their real condition (Flood, 1990). The artificial neuron receives the input signals and generates the output signals. Every data from the surrounding or an output from other neurons can be used as an input signal.

As follows, by applying Generalized Regression Neural Network (GRNN) specifically NeuralTools code from Palisade corporation, for data prediction in case of arch dam are shown. The data set used for training is basically values of the given measured data. In the training process, 70% of the data is used for training and 30% is used for validation. The variables are classified as independent or dependent, depending on their role in the prediction process. The dependent variable is the variable to be predicted. The independent variables are the “explanatory” variables used to predict the dependent variable. Cases where the dependent variable values are known are used to train and test a neural network.

The modeling by application of GRNN is based on the following variables: (1) water level in piezometer PZCB2 as dependent numeric value and water level in the reservoir as independent numeric value, (2) water level in piezometer PZCB3 as dependent numeric value and water level in the reservoir as independent numeric value, (3) seepage flow beneath the dam as dependent numeric value and water level in the reservoir as independent numeric value, (4) displacement in pendulum CB2 as dependent numeric value and water level and ambient temperature as independent numeric value, (5) displacement in pendulum CB3 as dependent numeric value and water level and ambient temperature as independent numeric value, and (6) crack opening in C4_C5 as dependent numeric value and water level and ambient temperature as independent numeric value.

4 CALIBRATION PROCESS OF THE DAM

The calibration process includes analysis of variables such as radial displacements (pendulums CB2 and CB3 in the central block of the dam), crack opening displacement (sensor C4-C5 at rock foundation interface), piezometric levels (PZCB2 and PZCB3 at rock-foundation interface) and seepage (weir at the downstream toe of the dam). The required calculated data are derived for corresponding nodes within the numerical model. The calibration process is carried out by comparison of the measured and calculated radial displacements at corresponding nodes for various variables of the FEM model respectively.

4.1 Calibration of pendulums displacements time series

By comparison of the radial displacements for pendulum CB2 by FEM analysis (Fig. 4) it can be noticed good matching of the data regarding the distribution and the values. The maximal measured values for pendulum CB2 range in interval from 15.95 mm to -27.48 mm, while the calculated values from 19.5 mm to -22.9 mm. The measured and calculated pendulums displacements time series are generally in correlation with the variation of the water level in the reservoir and air temperature. Namely, at higher water levels in the reservoir the displacements are in downstream direction (the hydrostatic pressure generates greater displacement then the temperature effect), while at lower water levels in the reservoir the displacements are in upstream direction, combined with the temperature effect that generates displacements in upstream direction.

By comparison of the radial displacements for pendulum CB2 by Neural Networks (NN) analysis (Fig. 6) it can be noticed good matching of the data regarding the distribution and the values. In case of radial displacements for pendulum CB3 by Neural Networks analysis (Fig. 5) it can be noticed excellent matching of the data regarding the distribution and the values. The interval of variation of the measured and calculated data for the displacements of pendulum CB2 is (-17.82÷19.41) mm, while the interval in case of pendulum CB3 is (-2.3÷2.3) mm. In analogy of the calculated data by FEM, and here the calculated displacements by Neural Networks models are

in correlation with the variation of the water level in the reservoir and air temperature (Fig. 6 and Fig. 7). Namely, at higher water levels in the reservoir the displacements are in downstream direction (the hydrostatic pressure generates greater displacement then the temperature effect), while at lower water levels in the reservoir the displacements are in upstream direction, by influence of the temperature effect that generates displacements in upstream direction.

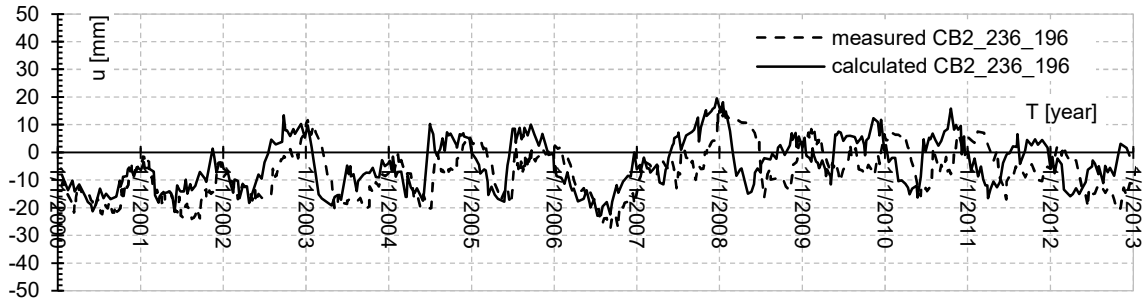


Figure 4. Display of measured and calculated time series of CB2 pendulums displacements for 2000-2012.

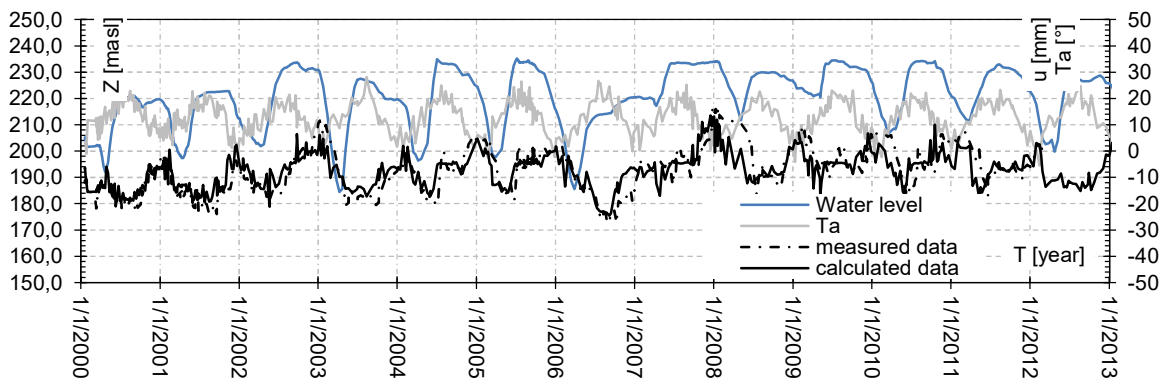


Figure 6. Display of measured and calculated time series of CB2 pendulums displacements for 2000-2012.

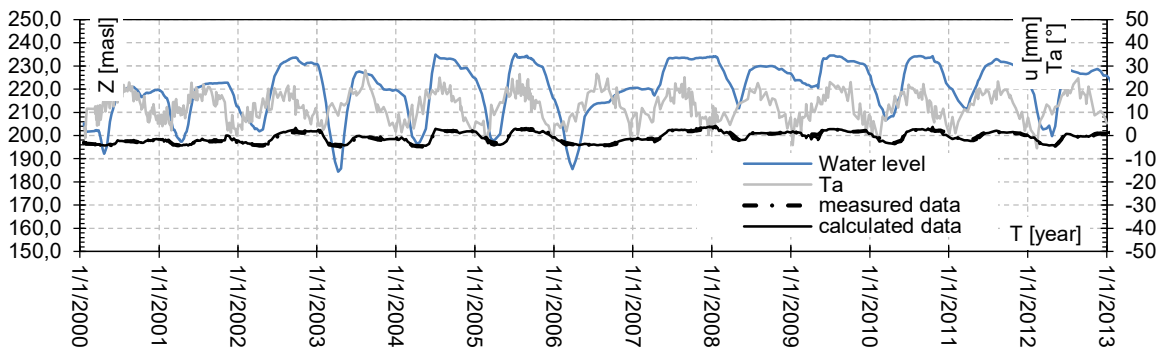


Figure 7. Display of measured and calculated time series of CB3 pendulums displacements for 2000-2012.

4.2 Calibration of crack opening time series

The calibration process for the crack opening displacements is carried out by numerical model with nonlinear constitutive law for concrete (Table 2). The calculated radial displacements as deduction of the radial displacements in the corresponding nodes are projected to sensor C4-C5 direction in order to obtain the variation values for the relative distance. On Fig. 8 are displayed calculated and measured relative distance for displacements in direction of the sensor C4-C5. It can be noticed that in general there is a similar distribution of the values for the calibration period, however there is a less good matching of the calculated and measured values. Namely, the calculated relative distance values are mainly lower than the measured values. The reason for such lower degree of matching of the values can be the stiff coupling condition at interface dam-foundation, modeled as kinematic constraint in the model. So a potential case to be investigated

is to model the contact dam-foundation by interface elements (with both linear and non-linear properties) combined with the variation of the stiffness properties of the rock (in central part and the banks) in order to improve the calibration process.

The measured and calculated values are mainly in reverse correlation with the water level in the reservoir apropos in period when the water level is low there is increase of the relative distance (positive values) while in period of higher water levels there is a decrease (negative values). Regarding the temperature, the displacement manifest more variable behavior apropos the applied temperature effect has lower influence the water level in the reservoir. The maximal measured relative distance values range in interval $(2.17 \div -2.43)$ mm, while the calculated values vary in range $(0.56 \div -0.65)$ mm.

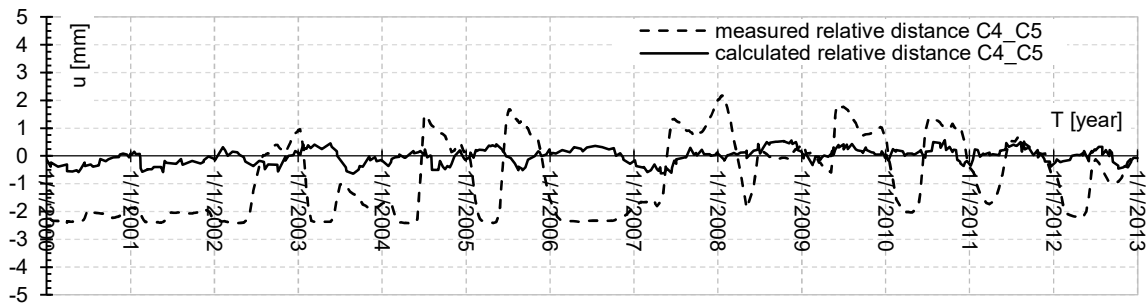


Figure 8. Display of calculated and measured time series of crack openings at sensor C4-C5 for 2000-2012.

On Fig. 9 are displayed calculated and measured data for the relative distance for displacements in direction of the sensor C4-C5 by applying Neural Networks model. An excellent matching for the distribution and the calculated values is obtained. This can be confirmed by the interval of variation of the measured and calculated data for the relative crack displacements of sensor C4-C5, in interval of $(-1.8 \div 2.4)$ mm. In opposite of the calculated data by FEM for sensor C4-C5, here the calculated relative crack displacements by Neural Networks models are in correlation with the variation of the water level in the reservoir and air temperature (Fig. 9). Namely, at higher water levels in the reservoir there is decrease of the relative crack displacements (negative values), while at low water levels there is increase of the relative crack displacements (positive values).

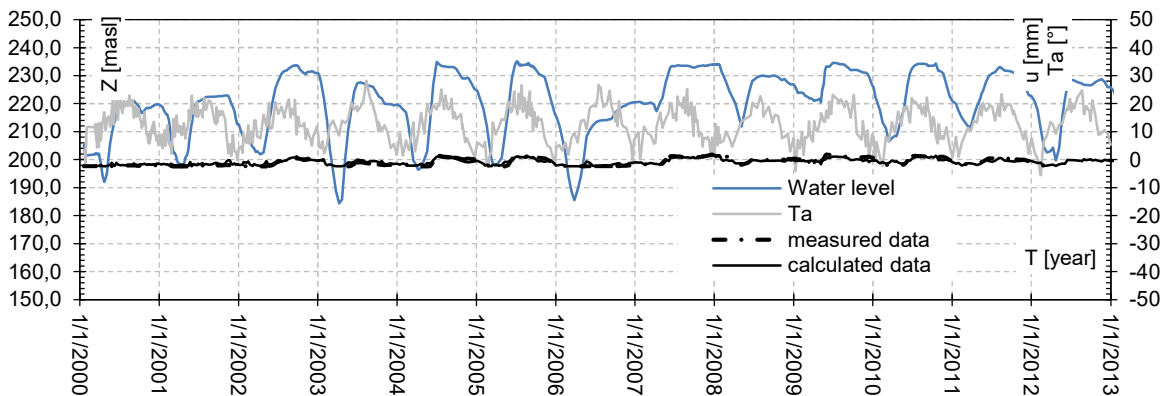


Figure 9. Display of calculated and measured time series of crack openings at sensor C4-C5 for 2000-2012.

4.3 Calibration of piezometric levels and seepage time series

The calibration process is carried out by plane (2D) numerical model for seepage analysis by modelling the foundation medium below the central block of the dam including running of load cases for full timeline period 2000-2012, and subsequent comparison of the measured and calculated piezometric levels at corresponding nodes for piezometers PZBC2 and PZBC3. The calculated piezometric levels are obtained by the values of the equipotential lines (H).

Numerical analysis of seepage flow in the foundation of the arch dam is carried out by plane (2D) model, where foundation with included grout curtain is modeled with plane elements. For

discretization of the dam body and the rock foundation is applied quadrilateral finite element, by 4 nodes. Namely, the model is composed of the rock foundation with included zone of grout curtain. The plane (2D) model has geometrical boundaries, limited to horizontal and vertical plane (Fig. 3), adopted according to the specified data [Malm & all, 2021]. The discretization is conveyed by including zones of various hydraulic parameters in the model – rock foundation and grout curtain, approximately modelling the rock foundation per 75m upstream and downstream of the dam.

However, the hydraulic properties for the material in the rock foundation were not available. So, the first step is to calibrate the value for the permeability coefficient k in accordance with the seepage values from the monitoring process for homogeneous rock foundation. The estimated permeability coefficient for laminated metamorphic slate ranges in interval $k=(10^{-7} \div 10^{-9})\text{m/s}$ [Lianyang, 2016, Fell et al, 2015]. The permeability coefficient additionally is calibrated by the value of the full seepage flow directly below the dam, specified as measured values in weir at gallery located at the downstream toe of the dam. So, according to the available measuring data for water level at 232.0 m the average registered seepage flow is 8 l/min. From the registered reservoir water levels and seepage flow it can be noticed general correlation, however in some periods there is discrepancy in the measured values that could be indication that the seepage flow is caused by additional influences then the seepage process in the rock foundation. The seepage analysis was carried out for $H=232.0$ m as upstream boundary condition and $H=0$ m as downstream boundary condition, by applying Darcy flow rule adopting the rock foundation as heterogeneous flow medium, composed of rock material (laminated metamorphic slate) and two sections (vertical and inclined) of grout curtain, by assumed permeability coefficient in first iteration $k_{rf}=1 \times 10^{-7}$ m/s for the rock zone.

By the initial calibration calculation of the permeability coefficient for homogeneous rock foundation was obtained value of $k=2.89 \times 10^{-8}$ m/s, applied in the calculation for the full calibration and prognosis analysis of the piezometric levels and seepage. Due to the grout curtain in the rock foundation (heterogeneous zone), additional calibration were carried out, in order to match the measured seepage flow $Q_m=8$ l/min and thus obtaining value of permeability coefficient for the rock foundation $k_{rf}=12.5 \times 10^{-8}$ m/s and permeability coefficient for the grout curtain $k_{gc}=2.5 \times 10^{-8}$ m/s, used as input parameters for the seepage calibration and prognosis stage.

By comparison of the calculated and measure seepage values (Fig. 10) it can be noticed good matching of the registered and calculated seepage flow data regarding the distribution and the values. Also, there is good matching apropos correlation of the registered reservoir water levels and registered and calculated seepage flow. The measured peak values of the seepage flow occur are approximately at normal water level so this may be indication for additional leakage occurrences that affect the seepage process. The measured seepage flow varies in interval $(0.01 \div 26.5)$ l/min, while the calculated values in interval $(0.001 \div 18)$ l/min. However, the occurred peak values of the seepage flow (especially in 2009) required additional explanation and research due to the very high values at approximately constant water level in the reservoir. Namely, they could occur due to another reason such as seepage zone in the dam or zones in the rock foundation that have higher permeability than the presumed. Additional calibration should include modelling of eventual more permeable zones in the rock foundation and more precise calibration of the permeability coefficient of the grout curtain.

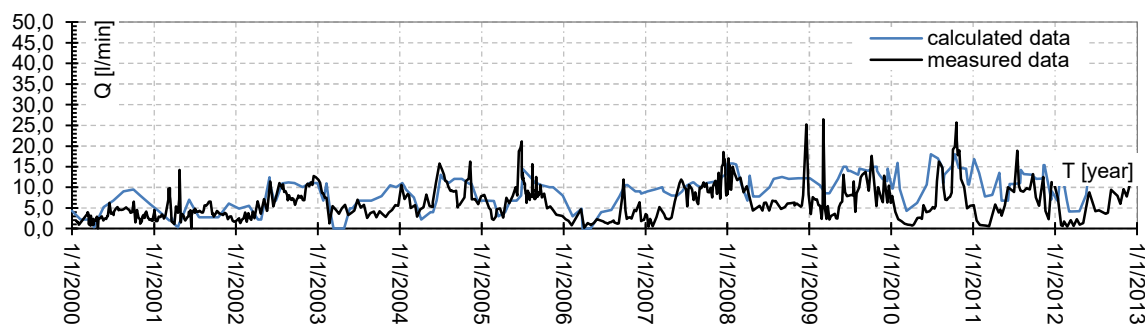


Figure 10. Display of measured and calculated seepage flow time series for period 2000-2012 by FEM.

By comparison of the piezometric levels for piezometers PZCB2, calculated by NN model (Fig. 11) it can be noticed excellent matching of the measured and calculated data regarding the distribution and the values. This can be confirmed by the interval of variation of the measured and calculated data for the piezometric levels for piezometer PZCB2, ranging in interval of $(-3.6 \div 2.9)$ masl. The calculated piezometric levels by NN model, in analogy of the calculated values from the FEM model for seepage analysis, are in correlation with the reservoir water level.

By comparison of the measured and calculated seepage flow values, obtained by the NN model (Fig. 12), it can be noticed not so good matching of the data regarding the distribution and the values. The calculated values are in some period lower than the measured values while in some periods are higher. The maximal measured seepage flow varies in interval $(0.01 \div 26.5)$ l/min, while the calculated values in interval $(0.37 \div 11.9)$ l/min. The interval of variation of the measured and calculated data for the seepage flow is ranging in interval $(-6.6 \div 21.6)$ l/min.

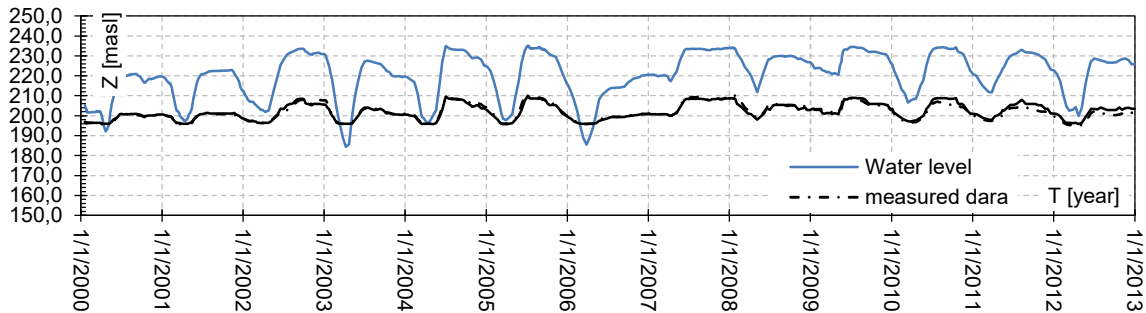


Figure 11. Display of measured and calculated piezometric levels for PZCB2 for period 2000-2012 by NN.

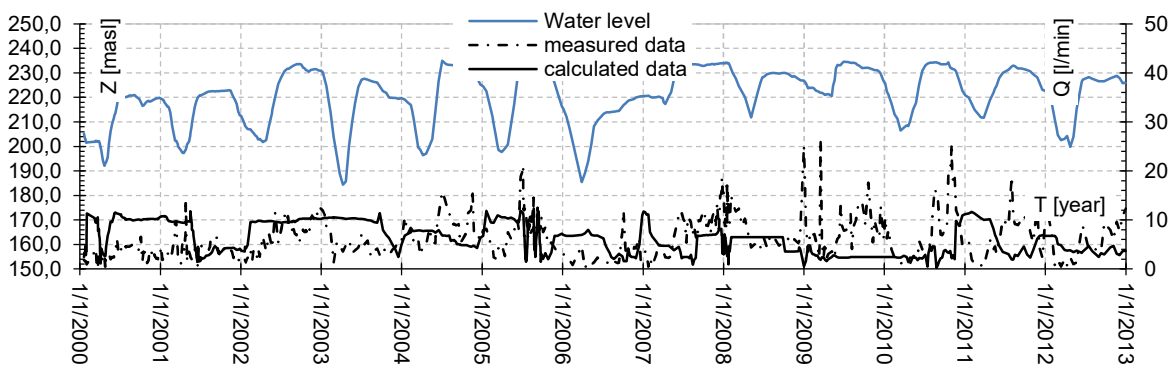


Figure 12. Display of measured and calculated seepage flow time series for period 2000-2012 by NN.

5 PREDICTION (PROGNOSIS) PROCESS OF THE DAM

5.1 *Prognosis of pendulums displacements time series*

The prognosis stage consists of short-term and long-term prediction of the specified variables. Namely, the short-term prediction includes period January, 2013-June, 2013, while the long-term prediction captures period July, 2013-December, 2017. The prognosis process is carried out by numerical model including running of full time steps for the time series within the short-term period. The prognosis process for the long-term behavior is carried out by numerical model including running of appropriate representative load cases for the time series.

The calculated displacements for pendulum CB2 (Fig. 13), calculated by FEM model, for the short-term prognosis are mainly in upstream direction, maximal value of -16.3 mm, while the maximal displacement in the downstream direction is 1.75 mm. The calculated displacements for pendulum CB3 for short-term period are mainly in downstream direction, with maximal value of 1.7 mm and maximal value of -0.3 mm in downstream direction. The calculated values for pendulum CB2 are in correlation with the water level apropos the lowering of the water level within the short-term period is dominant factor that enables modus for manifestation of the displacements in the upstream direction while the applied temperature effect has lower influence

on the displacements. In case of pendulum CB3 the lowered water level and temperature does not generate significant variation of the displacements values.

The calculated displacements for pendulum CB2 (Fig. 13), calculated by FEM model, for the long-term prognosis are also mainly in upstream direction, maximal value of -24.6 mm, while the maximal displacement in the downstream direction is 10.5 mm. The calculated displacements for pendulum CB3 for the long-term period are mainly in downstream direction, with maximal value of 2 mm and maximal value of -0.55 mm in downstream direction. The calculated values for pendulum CB2 are mainly in correlation with the water level apropos the lowered water level within the long-term period is contributing factor that enables modus for manifestation of the displacements in the upstream direction while the applied temperature effect has lower influence on the displacements. In case of pendulum CB3 the lowered water level and temperature does not generate significant variation of the displacements values.

The calculated displacements for pendulum CB3 (Fig. 14), calculated by NN, for the short-term prognosis are mainly in upstream direction, maximal value of -4.3 mm, while the maximal displacement in the downstream direction is 1.4 mm. The calculated values for pendulum CB3 are mainly in correlation with the water level apropos the lowering of the water level within the short-term period is dominant factor that enables modus for manifestation of the displacements in the upstream direction while the applied temperature effect has lower influence on the displacements. The calculated displacements for pendulum CB3 (Fig. 14), by NN model, for the long-term prognosis are also mainly in upstream direction, maximal value of -4.5 mm, while the maximal displacement in the downstream direction is 1.6 mm. The calculated values for pendulum CB3 are mainly in correlation with the water level apropos the lowered water level within the long-term period is contributing factor that enables modus for manifestation of the displacements in the upstream direction while the applied temperature effect has lower influence on the displacements. In case of pendulum CB3 the lowered water level and temperature does not generate significant variation of the displacements values.

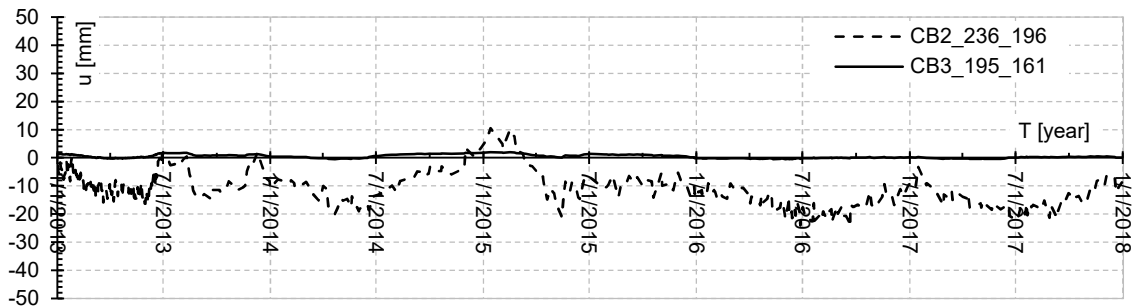


Figure 13. Display of calculated prognosis time series of pendulum CB2 and CB3 displacements for 2013-2017 by FEM.

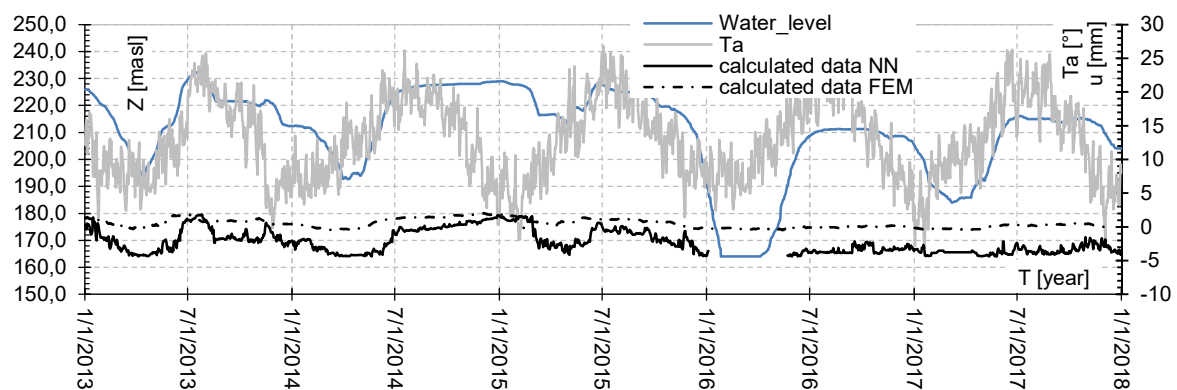


Figure 14. Display of calculated prognosis time series of pendulum CB3 displacements for period 2013-2017 by FEM and NN.

5.2 Prognosis of crack opening time series

The prognosis process is carried out by numerical model including running of full time steps for the time series within the short-term period. The prognosis process for the long-term behavior is carried out by numerical model including running of appropriate representative load cases for the time series. The calculated relative distance for the short-term prognosis at sensor C4-C5 are varying from increase (positive values) to decrease (negative) values (Fig. 15). The maximal calculated values are -0.5 mm and 0.3 mm respectively. The calculated values are in correlation with the water level apropos at higher water level the crack displacements are increasing while at lowered water level they are decreasing. Very similar case is also with the applied temperature effect apropos lowering of the temperature in the short-term period lowers the crack displacements. The calculated relative distance for the long-term prognosis at sensor C4-C5 are less varying from increase (positive values) and decrease (negative) values apropos mainly manifest decrease of the crack openings. The maximal calculated values are -0.72 mm and 0.56 mm respectively. The calculated values are in correlation with the water level apropos at longer period of higher water level the crack displacements are increasing while at lowered water level they are decreasing. Very similar case is also with the applied temperature effect apropos lowering of the temperature in the long-term period lowers the crack displacements.

The prognosis process is carried also out by Neural Networks model for the time series within the short-term and the long-term. The calculated relative distance for the short-term prognosis at sensor C4-C5, calculated by NN model, are varying mainly to decrease (negative) values (Fig. 16). The maximal calculated values are -2.5 mm and 0.1 mm respectively. The calculated values are in correlation with the water level apropos at higher water level the crack displacements are increasing while at lowered water level they are decreasing. Very similar case is also with the applied temperature effect apropos lowering of the temperature in the short-term period lowers the crack displacements. The calculated relative distance for the long-term prognosis at sensor C4-C5, by NN model, are also mainly decrease zone (negative) values apropos mainly manifest decrease of the crack openings. The maximal calculated values are -2.35 mm and 0.1 mm respectively. The calculated values are in correlation with the water level apropos at longer period of higher water level the crack displacements are increasing while at lowered water level they are decreasing. Very similar case is also with the applied temperature effect apropos lowering of the temperature in the long-term period lowers the crack displacements.

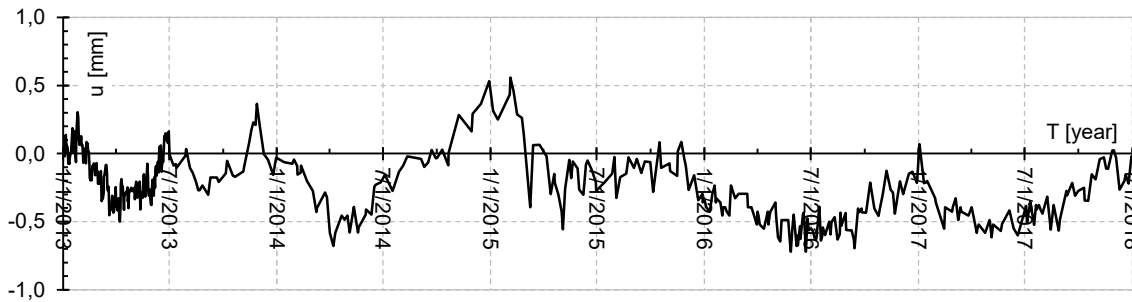


Figure 15. Prognosis calculated time series of C4-C5 relative distance for period 2013-2017 by FEM.

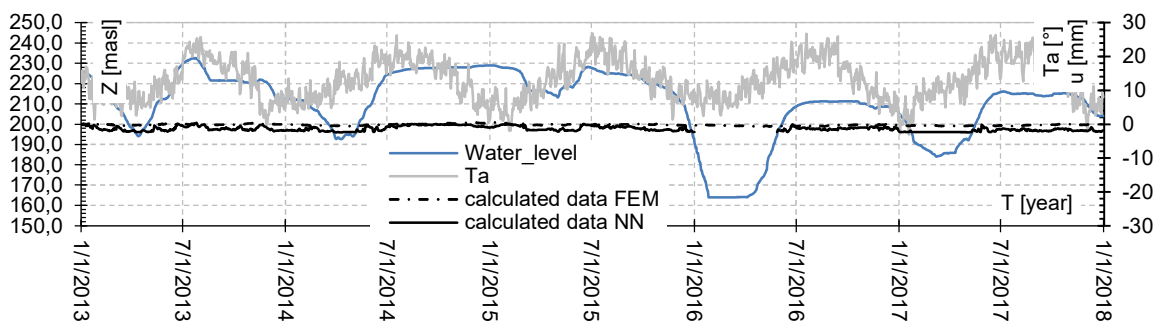


Figure 16. Prognosis calculated time series of C4-C5 relative distance for 2013-2017.

5.3 Prognosis of piezometric levels time series

The prognosis process for piezometric levels for PZCB2 is carried out by NN numerical model for seepage analysis. The calculated piezometric levels for piezometer PZCB2 for the short-term and long term prognosis, as expected, are varying in correlation with the water level in the reservoir (Fig. 17). The maximal and minimal calculated values for the piezometric levels are respectively 205.5 m and 195.5 m.

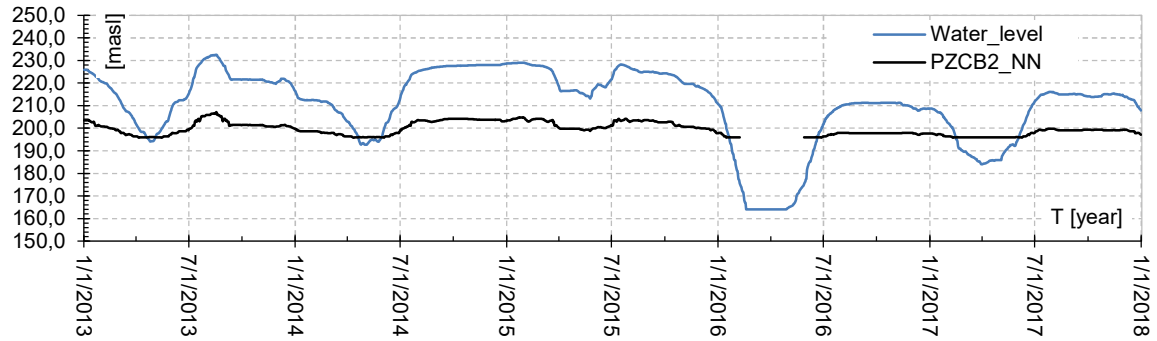


Figure 17. Prognosis calculated time series of piezometric levels for PZCB2 for 2013-2017 by NN model.

5.4 Prognosis of seepage time series

The calculated seepage flows for the short-term and long term prognosis, calculated by FEM model, as expected, are varying in correlation with the water level in the reservoir (Fig. 18). The maximal and minimal calculated values for the seepage flow are respectively 3.34 l/min m and 0.06 l/min. The calculated seepage flows for the short-term and long term prognosis, calculated by NN model, as expected, are varying in correlation with the water level in the reservoir (Fig. 19). The maximal and minimal calculated values for the seepage flow are respectively 11 l/min m and 0.1 l/min.

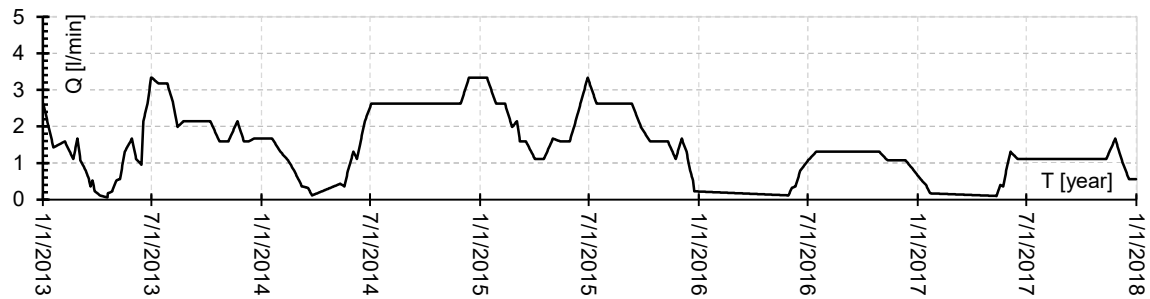


Figure 18. Prognosis calculated time series of seepage flow for Jan,2013-Dec,2017 by FEM model.

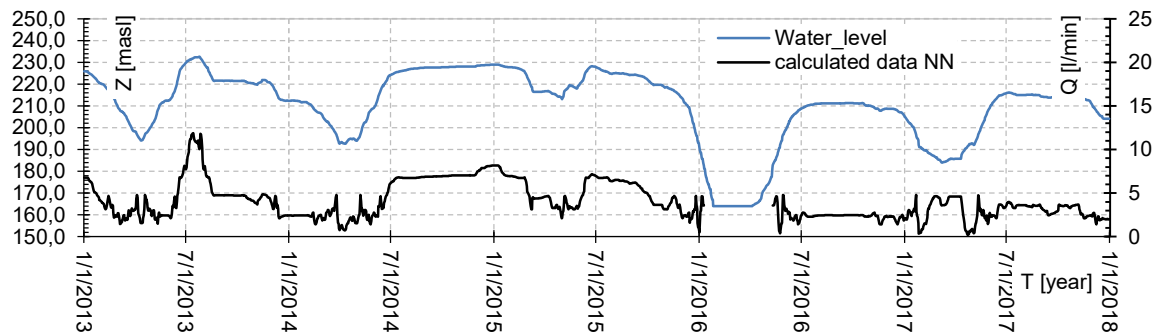


Figure 19. Prognosis calculated time series of seepage flow for Jan,2013-Dec,2017 by NN model.

6 CONCLUSIONS

The behavior of the dam during the service period for variation of the water levels in the reservoir and temperature effect was simulated by application of the Finite Element Method with spatial (3D) numerical model and Neural Networks model. The numerical analysis was carried out by taking in consideration the specified data for the numerical model (fully reproduced according to the formulation data) and variations of the water level in the reservoir and the air temperature, by applying coupled thermo-mechanical analysis of the dam in static conditions. The loading scenarios for calculation of the required variables were adopted according to the extreme values for the available monitoring records of the variables and records for reservoir water levels and air temperature by coupled thermo-mechanical analysis of the dam and hydraulic analysis of the seepage process.

The prediction of the behavior of the dam was analyzed in two stages – calibration and prognosis stage. From the carried out numerical experiment by FEM model for calibration and prediction of the behavior of the dam EDF, following conclusions and recommendations are derived:

- (1) The calibration process of the measured and calculated radial displacements for pendulum CB2 provided good matching of the data regarding the distribution and the values. In case of pendulum CB3 a good matching of the data regarding the distribution and some less good matching of the data regarding the values is obtained.
- (2) The calibration process for the relative distance C4-C5, in general, has a good matching of the distribution of the values, however there is a difference in the calculated and measured values (the calculated relative distance values are mainly lower than the measured). The measured and calculated values are mainly in reverse correlation with the water level in the reservoir apropos in period when the water level is low there is increase of the crack opening (positive values) while in period of higher water levels there is a decrease (negative values). Regarding the temperature, the displacements manifest less variable behavior apropos the applied temperature has lower influence on the displacements.
- (3) By comparison of the calculated and measured piezometric levels for piezometers PZCB2 and PZCB3 as well and the seepage flow is obtained good matching of the records regarding the distribution and less good matching regarding the values.
- (4) The calculated displacements for pendulum CB2 prognosis period are mainly in upstream direction, while the calculated displacements for pendulum CB3 are mainly in downstream direction. The calculated values for pendulum CB2 are mainly in correlation with the water level apropos the lowered water level while the applied temperature effect has lower influence on the displacements. In case of pendulum CB3 the lowered water level and temperature does not generate significant variation of the displacements values.
- (5) The calculated relative distance for the prognosis period at sensor C4-C5 are varying from increase (positive values) to mainly decrease (negative) values. The calculated values are in correlation with the water level apropos at higher water level the crack displacements are increasing while at lowered water level they are decreasing. Very similar case is also with the applied temperature effect apropos lowering of the temperature in the short-term period lowers the relative distance C4-C5.
- (6) The calculated piezometric levels for piezometer PZCB2, PZCB3 and seepage flow data for short and long term prognosis stage, are varying in correlation with the reservoir water level.
- (7) Improved calibration should be carried out apropos the case to be analyzed is to model the contact dam-foundation by interface elements (by linear and non-linear properties) combined with the variation of the stiffness properties of the rock (in central part and the banks).

The prediction of the behavior of the dam was analyzed in two stages – calibration and prognosis stage. From the carried out numerical experiment by NN model for calibration and prediction of the behavior of the dam EDF, following conclusions and recommendations are derived:

- (1) The calibration process of the measured and calculated radial displacements for pendulum CB2 provided relatively good matching of the data regarding the distribution and the values. In case of pendulum CB3 a very good matching of the data regarding the distribution and the values was obtained.

- (2) The calibration process for the relative distance C4-C5, in general provided excellent matching of the distribution and the values. The calculated values are in correlation with the reservoir water level and the temperature.
- (3) By comparison of the calculated and measured piezometric levels for piezometers PZCB2 and PZCB3 is obtained very good matching of the records regarding the distribution and the values. In case of the seepage flow less good matching of the data regarding the distribution and the values was obtained.
- (4) The calculated displacements for pendulum CB2 and CB3 prognosis period are mainly in upstream direction. The calculated values for pendulum CB2 and CB3 are mainly in correlation with the water level apropos.
- (5) The calculated relative distance for the prognosis period at sensor C4-C5 are varying mainly to decrease (negative) values of crack openings.
- (6) The calculated piezometric levels for piezometer PZCB2 and PZCB3 and seepage flow for the short-term and long term prognosis, are varying in correlation with the water level in the reservoir.
- (7) The overall behavior of the concrete arch dam, taking in consideration the findings from the calibration and the prognosis stage, is within the expected mode for such structure.
- (8) According to the measured and calculated values for the variables by NN model, warning levels corridors are defined by applying criteria of $3 \times \sigma$, where σ is standard deviation of absolute error, generated by the NeuralTools code.
- (9) General conclusion can be drawn out for the analysis task that Neural Network model provided improved matching of the calculated vs measured data for all variables compared with the FEM model.
- (10) The conclusion from the both numerical experiments (FEM and Neural Networks) is that the dam behavior, with adopted geometry and material, is within the expected mode.

REFERENCES

- Flood, I. (1990). Simulating the construction process using neural networks. Proceedings of the 7th ISARC - International association for Automation and Robotics in Construction. Bristol.
- Flood, I. C. P. (1996). Modeling construction processes using artificial neural networks. *Automation in Construction*, 4(4), 307-320.
- Flood, I. K. N. (1994). Neural networks in civil engineering II: Systems and application. *Computing in Civil Engineering*.
- Malm, R. & all, 2021. Theme A, Formulation, 16th International Benchmark Workshop on Numerical Analysis of Dams, Ljubljana, Slovenia.
- Mitovski S., 2015a. PhD thesis, Static analysis of concrete dams by modeling of the structural joints, Ss Cyril and Methodius University in Skopje, Civil Engineering Faculty
- Mitovski S., Dimov L., Petkovski L., 2017b. "Comparison of calculated and survey monitoring displacements for St. Petka dam", *Scientific Journal of Civil Engineering* (ISSN-1857-839X), Volume 6, Issue 2.
- Mitovski S., Kokalanov G., Petkovski L., 2017a. Numerical analysis on St. Petka dam, 4th Congress on dams, Struga, N. Macedonia.
- Mitovski S., Kokalanov G., Petkovski L., Tancev L. and Veleski G., 2017b. "Static and seismic analysis of an arch-gravity dam" 14th ICOLD International Benchmark Workshop on Numerical Analysis of Dams, Stockholm, Sweden.
- Mitovski S., Petkovski L., Kokalanov G., 2015b. Safety evaluation of an arch dam by calibrating numerical models and monitoring data, SMAR2015 – Third Conference on Smart Monitoring, Assessment and Rehabilitation of Civil Structures, Antalya, Turkey.
- Novak P. et all, 2007. "Hydraulic structures", Taylor & Francis Group, London.
- P.V. Lade, 1984. Failure Criterion for Frictional Materials in *Mechanics of Engineering Materials*, Chap 20 (C.s.Desai,R.H.Gallagher ed.) Wiley & Sons.
- Robbin Fell, Patrick MacGregor, David Stapledon, Graeme Bell, Mark Foster. (2015). *Geotechnical engineering of dams*. London, UK: CRC Press Taylor & Francis Group.
- SOFiSTiK Manual, 2022.
- Tanchev L., 2014. Dams and appurtenant hydraulic structures, Second edition, A.A. Balkema Publ., CRC press, Taylor & Francis Group plc, London, UK.
- USBR, 1977. Design of arch dams,
- Zhang Lianyang, 2016. Engineering properties of rocks, Elsevier Ge-Engineering Book Series, Series Editor John A. Hudson, Vol. 4.

BEHAVIOUR OF EARTH DAM DURING RESERVOIR FILLING AND EARTHQUAKE ACTION, DAM IN SLOVENIA

Ljupcho Petkovski

Faculty of Civil Engineering, Ss. Cyril and Methodius University in Skopje, North Macedonia

Stevcho Mitovski

Faculty of Civil Engineering, Ss. Cyril and Methodius University in Skopje, North Macedonia

Frosina Panovska

Faculty of Civil Engineering, Ss. Cyril and Methodius University in Skopje, North Macedonia

ABSTRACT: In the static analysis of the earth zoned dam in Slovenia, for the state of rapid filling of the reservoir and lowering of the level for remediation of the dam, up to the state of long-term maintenance at normal level, which is a pre-earthquake state, an elastoplastic model with variable modulus of elasticity was used, for the local materials in the dam body. The analysis was performed in drained conditions with effective stresses, using combined mechanical and seepage analysis in the time domain. Criterion for calibration of nonlinear elastic material parameters is the condition that the horizontal displacements in the dam crest, for the condition of the first filling of the reservoir, are approximately the same with the measured values, i.e. about -120 mm in the downstream direction. The key conclusion from the static analysis is that the embankment dam, with the adopted geometry and composition of materials, possesses satisfactory static stability. In the analysis of the dynamic response of the dam, a nonlinear model is applied (equivalent linear analysis with inelastic material parameters), where the local materials are approximated with a variable maximum shear modulus. Permanent displacements during seismic excitation are determined by dynamic deformation analysis, where from the difference of the effective stresses in two successive time steps, incremental forces are determined, which result in corresponding deformations. The dynamic analysis confirms the seismic resistance of the embankment dam in the action of a design earthquake with PGA of 0.30 g, i.e. there is no danger of rapid and uncontrolled reservoir emptying, because the crest settlements from dynamic inertial forces for the duration of the earthquake are 1.1 m, apropos are much lower than the height above the normal level in the reservoir till dam crest, which is 3.2 m.

1 MODEL OF THE DAM AND MATERIAL PARAMETERS FOR STRUCTURAL ANALYSIS

1.1 Basic characteristics of the analyzed dam

The representative cross-section, the parameters of the local materials for the embankment dam in Slovenia and the measured values from the dam monitoring are taken from the available data base [1]. The earth zoned dam with a clay core was built in 1985. It is founded on a rock foundation of Eocene flysch, which is practically waterproof and with high stiffness. The basic geometric characteristics of the dam and reservoir, Figure 1, are the following: crest elevation at 102.0 m.a.s.l., elevation of rock foundation 67.4 m.a.s.l., structural height 34.6 m, crest width 5.0 m, elevation at normal level 98.8 m.a.s.l. and elevation at minimum level 80.0 m.a.s.l.

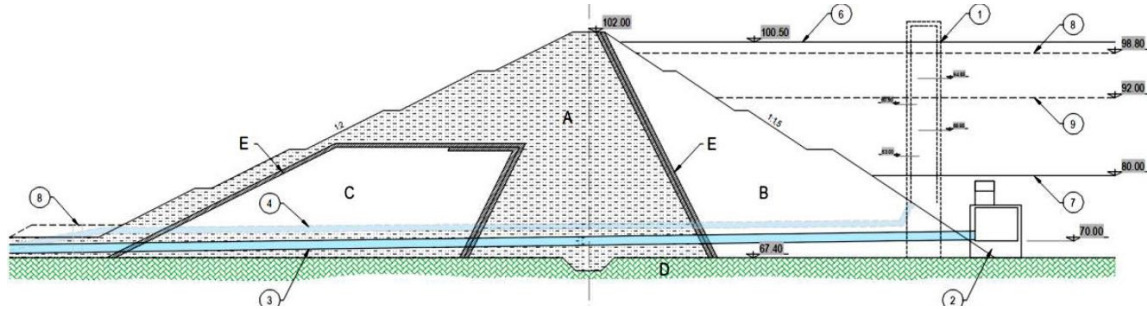


Figure 1. Representative cross-section of the earth dam.

1.2 Basic geomechanical parameters of the materials

The basic geomechanical parameters of the local materials are systematized in Table 1. The values from the available database are with a yellow background, and the other values are determined or assumed, according to the description of the materials.

Table 1. Material parameters.

Zone		A1	A2	B	C	D	Comment
dam structure		top of dam	core	upstream part	downstream part	bedrock	
material		gravel, silt	clayey silt	rockfill	rockfill and sand	Flysch	
γ_{spec}	kN/m ³	21.0	19.5	24.0	24.0	25.0	specific unit weight
γ_{dry}	kN/m ³	16.4	12.8	21.0	20.0	24.0	dry unit weight
n		0.219	0.344	0.125	0.167	0.040	void
e		0.280	0.523	0.143	0.200	0.042	void ratio
ω_{sat}	%	13.1	26.3	5.8	8.2	1.6	saturated wetness
$\omega < \omega_{\text{sat}}$	%	13.0	26.0	3.0	7.0	1.5	natural wetness
γ_{sat}	kN/m ³	18.5	16.2	22.2	21.6	24.4	saturated unit weight
γ	kN/m ³	18.5	16.1	21.6	21.4	24.4	natural unit weight
ϕ	o	36.0	0.0	38.0	38.0	39.0	angle of internal friction
c or c_u	kN/m ²	36.0	75.0	0.0	0.0	32.0	cohesion
k_s	m/s	1.0E-06	1.00E-09	1.0E-03	1.0E-04	1.0E-09	coefficient of permeability - secondly

k_d	m/d	8.6E-02	8.6E-05	8.6E+0 1	8.6E+0 0	8.6E-05	coefficient of permeability - daily
$K_0(\phi)$		0.41	1.00	0.38	0.38	0.37	at-rest earth pressure coefficient
$\nu(K_0)$		0.29	0.50	0.28	0.28	0.27	Poisson coefficient
ν		0.35	0.45	0.30	0.30	0.25	Poisson coefficient
M_v	kN/m ²	15,000	5,000	50,000	50,000		modulus of compressibility
m_v		6.67E-05	2.00E-04	2.00E-05	2.00E-05		coefficient of compressibility
E	kN/m ²	9,346	1,318	37,143	37,143	620,000	Young's modulus of elasticity

1.3 Mathematical model of the dam

In the mathematical model for simulating the behavior of the earth dam during the filling of the reservoir and the earthquake action, Figure 2, four different local materials are provided in the body of the dam, while the rock foundation at the base below the dam is adopted as non-deformable zone (due to the large difference in the stiffness properties) and also waterproof (due to the low coefficient of permeability). The justification for such approximation is confirmed by comparing models with and without rock foundation, for the state of reservoir filling, whereby a negligible difference in the state of stresses and deformations in the dam body is ascertained. Therefore, in order to avoid the bulkiness of the numerical model and the possible negative impact in the numerical experiments, all further analyzes are conveyed with a mathematical model where the rock foundation is not included.

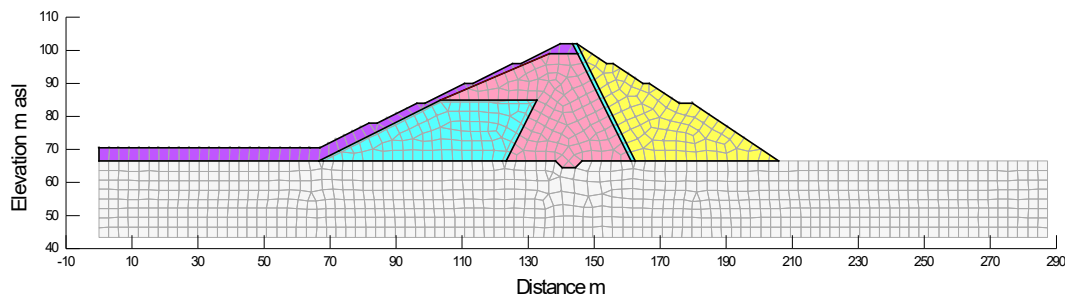


Figure 2. Mathematical model of the dam, discretized with 1,229 nodes and 1,147 elements.

2 SIMULATION OF DAM BEHAVIOR IN EXPLOITATION PERIOD

2.1 Stages of earth dam loading

The behavior of the dam in the service period is simulated with a mathematical model in real time domain, appropriate to the measured values from the technical monitoring. This ensures that the initial load state in the current load state is taken over from the previous stress state. The analyzes were performed using the effective stresses, apropos by tracking the increase and dissipation of the pore pressure with a coupled mechanical and hydraulic response with non-steady seepage in drained conditions.

The loading stages of the earth dam are systematized in Table 2. The monitoring of the dam behavior is simulated in a period of 33.54 years, from the beginning of the first filling of the reservoir, until the state of long-term maintenance at a normal level.

Table 2. Stages of loading of the earth dam.

Stage No.	description	from		to		dZ	Dt	dZ/Dt	Dt
		m asl	yyyy-mm-dd	masl	yyyy-mm-dd	m	days	m/d	years
1	first filling	81.84	1988-04-25	98.34	1990-04-17	16.50	722	0.023	1.977
2	to normal level	98.34	1990-04-17	98.80	1990-04-27	0.46	10	0.046	0.027
3	normal level	98.80	1990-04-27	98.80	2008-01-01	0.00	6,458	0.000	17.681
4	to emergency level	98.80	2008-01-01	92.00	2008-05-17	-6.80	137	-0.050	0.375
5	emergency level	92.00	2008-05-17	92.00	2018-05-17	0.00	3,652	0.000	9.999
6	to remediation level	92.00	2018-05-17	82.00	2018-12-06	-10.00	203	-0.049	0.556
7	remediation level	82.00	2018-12-06	82.00	2019-12-06	0.00	365	0.000	0.999
8	to normal level	82.00	2018-12-06	98.80	2019-11-08	16.80	337	0.050	0.923
9	normal level	98.80	2019-11-08	98.80	2020-11-07	0.00	365	0.000	0.999
10	earthquake	98.80	2020-11-07	98.80			12,249		33.54

2.2 Initial stress state prior to the first filling

The data from the monitoring of the dam are given for the first filling of the reservoir from elevation 81.84 m. Therefore, the initial stress state is determined for steady seepage through the dam for water level elevation dam at 81.84 m.a.s.l., Figure 3, by application of Seep/W program [2]. For this state of seepage pore pressure, the distribution of effective stresses in the dam body is determined, Figure 4, by application of Sigma/W program [3]. The coefficient of slope stability of the upstream slope is calculated with the realized stresses by application of program Slope/W [4] and is $F = 1.33$, apropos it is greater than the required 1.3, for temporary load.

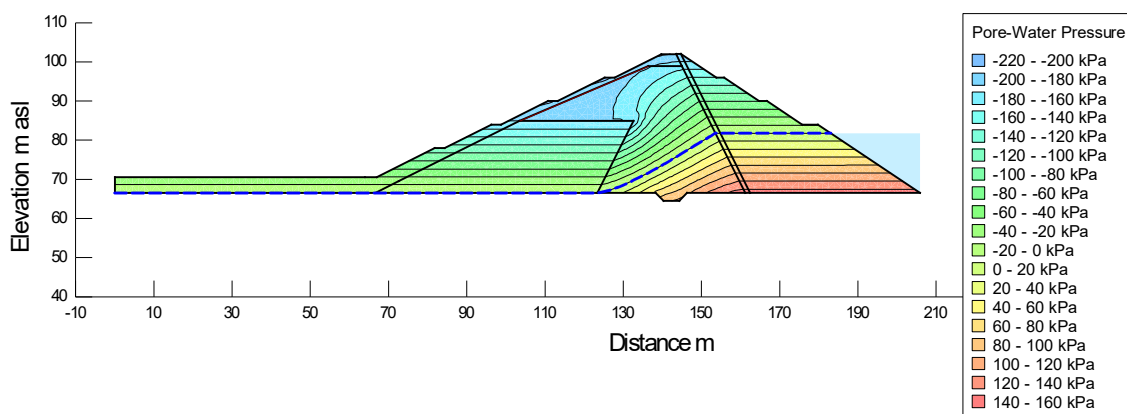


Figure 3. Initial state prior to the filling of the reservoir, distribution of pore pressure for steady seepage.

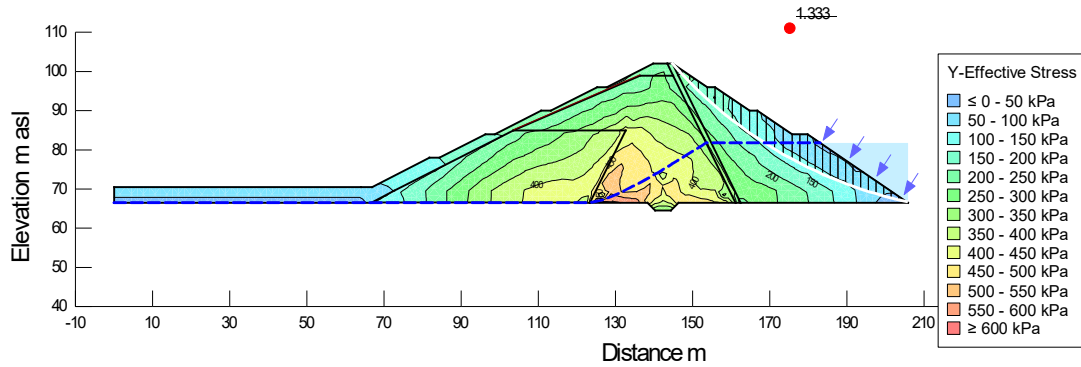


Figure 4. Initial state prior to the filling of the reservoir, distribution of vertical effective stress with coefficient of slope stability on the upstream slope $F=1.33$.

2.3 First filling of the reservoir and calibration of nonlinear material parameters

The first filling (or Stage 1) is simulated in 722 linear increments over a period of 722 days, according to the dynamics of the registered values from the technical monitoring, Figure 5.

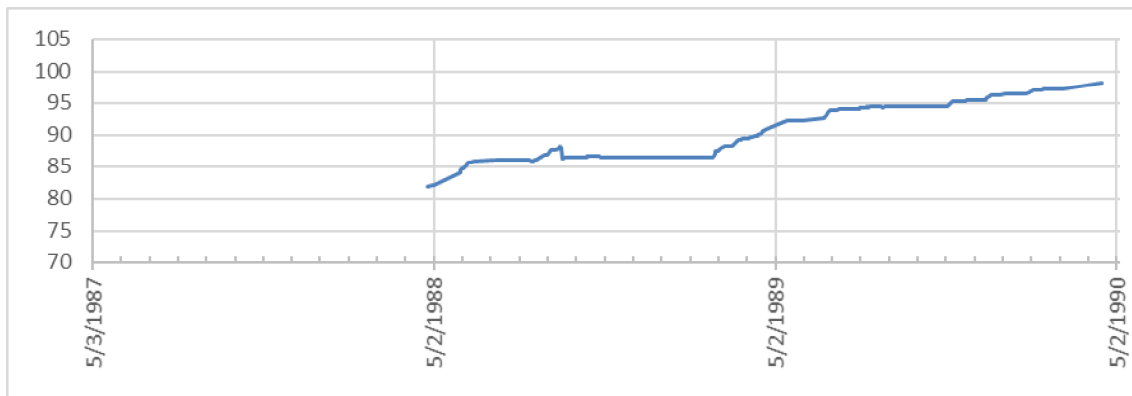


Figure 5. Dynamics of first filling of the reservoir, in m asl.

In the static analysis, for the local materials in the dam body, an elastoplastic model with variable modulus of elasticity $E = E(\sigma_y')$, Figure 6, with calibrated elastic parameters, is applied. Criterion for calibration is the condition that the horizontal displacements in the dam crest, for the state of the first filling of the reservoir, to be approximately same with the measured values, figure 7, i.e. about -120 mm in the downstream direction.

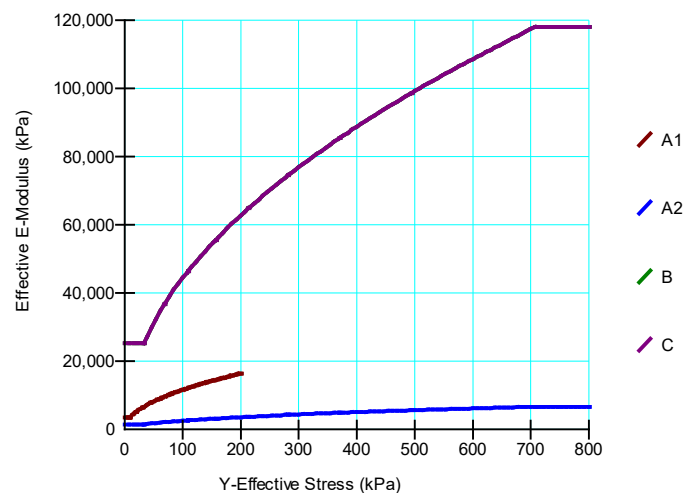


Figure 6. Calibrated values for variable elasticity modulus $E=E(\sigma_y')$ for the local materials in the dam body.

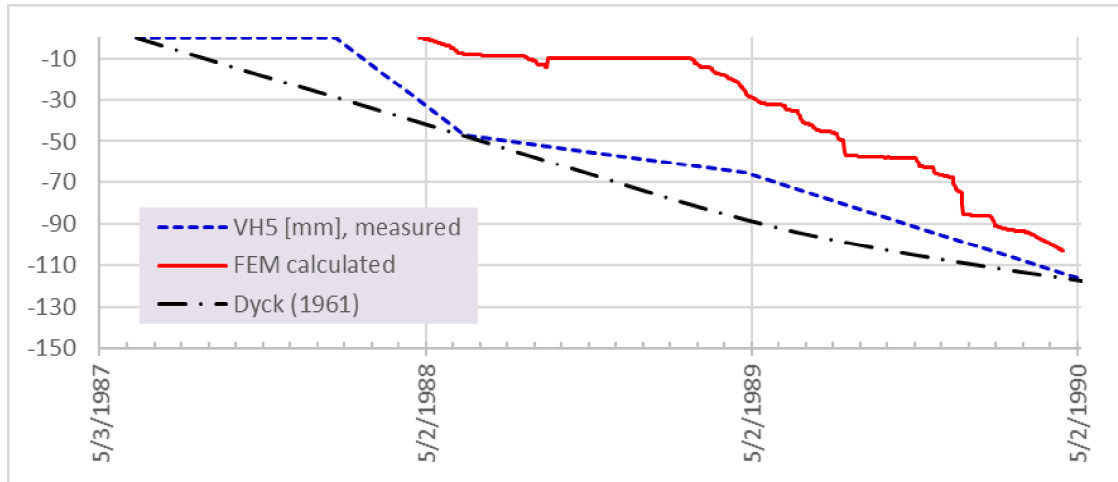


Figure 7. Comparison of calculated and measured horizontal displacements in mm (- downstream direction), in the dam crest (measuring point V5) during the first filling of the reservoir.

In all materials for construction of embankment dams, there is a dependence between stresses, deformations and time. That is, the materials show viscous behavior, and long-term loads on the viscous materials cause significant deformations called "creep" of the material. Figure 7 also shows the secondary horizontal displacements calculated by method of Dyck (1961). The following expression is used to calculate the secondary displacements at the embankment dams after the construction of the dam and the filling of the reservoir:

$$W = \frac{\varepsilon_t H}{100} \quad (1)$$

$$\varepsilon_t = \varepsilon_a + \alpha \ln t \quad (2)$$

Whereas, (W) is displacement in meters, (t) past period in years, (H) is height of dam above terrain, and coefficients (ε_a) and (α) depend on the type of dam and type of displacement.

Horizontal secondary displacements in the direction of the action of hydrostatic pressure are correlated with settlements caused by creep and, according to some authors, their value is about 50% of vertical displacements. Thus, if the mechanical response with the FEM and the empirical concept obtained horizontal displacements in the downstream direction of about 120 mm, the vertical settlement would be approximately 240 mm. For the values of the vertical rising in the crest obtained by the mechanical response with FEM of +150 mm, Figure 8, summed with the vertical creep settlement of -240 mm, we obtain approximately -90 mm, i.e. approximately to the measured settlement of around -100 mm.

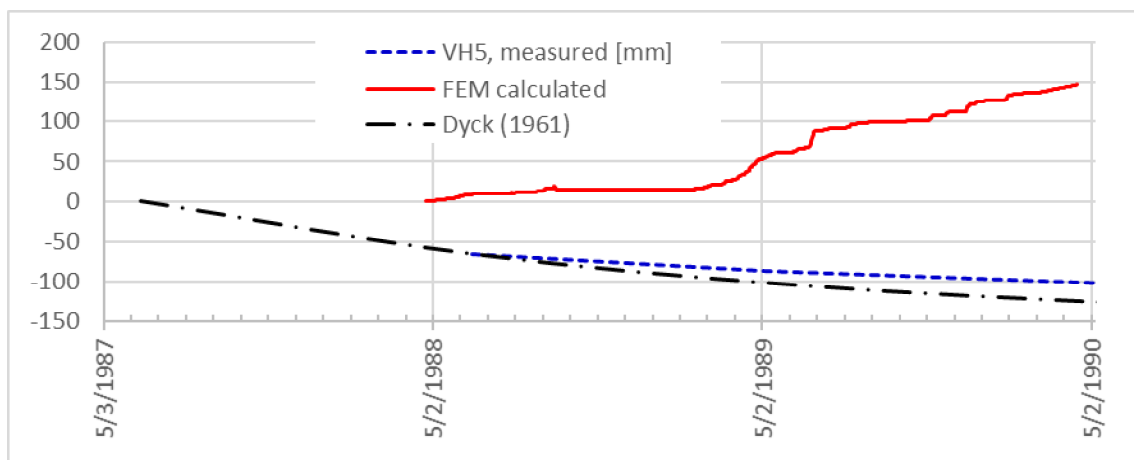


Figure 8. Comparison of calculated and measured vertical displacements in mm (+ elevation, - settlement), in the dam crest (measuring point V5) during the first charge of the reservoir.

2.4 Variation of the water level in the reservoir

The dam states during the variations of the water level in the reservoir from stage 2 to stage 9 (Table 2) are simulated in the time domain of the following numerical experiments:

- Stage 2, raising to normal level with 10 linear increments over a period of 10 days;
- Stage 3 maintenance of normal level with 60 exponential increments over a period of 6,458 days;
- Stage 4 lowering to emergency level with 20 linear increments in a period of 137 days;
- Stage 5 maintenance of emergency level with 30 exponential increments in a period of 3,652 days;
- Stage 6 lowering to remediation level with 30 linear increments over a period of 203 days;
- Stage 7 maintenance of remediation level with 15 exponential increments for a period of 365 days;
- Stage 8, raising to normal level with 30 linear increments over a period of 337 days and
- Stage 9 maintenance at a normal level with 15 exponential increments over a period of 365 days.

The comparison of the estimated (with FEM model and empirical) and the measured horizontal and vertical displacements in the dam crest are shown in Figures 9 and 10.

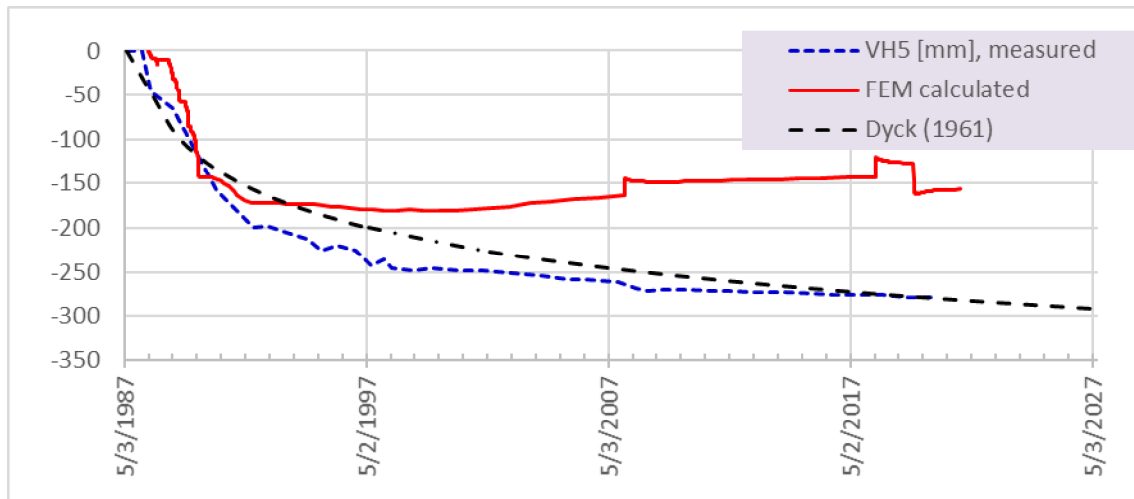


Figure 9. Comparison of calculated and measured horizontal displacements in mm (- downstream), in the dam crest (measuring point V5), during Stage 1 to Stage 9.

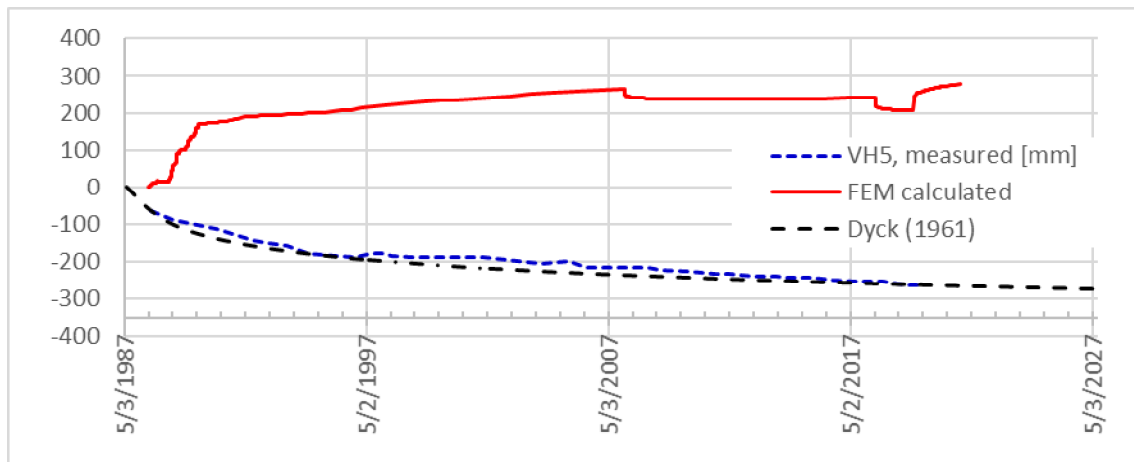


Figure 10. Comparison of calculated and measured vertical displacements in mm (+ elevation, - settlement), in the dam crest (measuring point V5), during Stage 1 to Stage 9.

By extrapolating the displacements in the crest until 2027, under the proper behavior of the dam, a horizontal downstream displacement of 300 mm and a settlement of approximately 300 mm can be treated.

The stress state in the final stage or stage 9, Figure 11, is the initial pre-earthquake state. The coefficient of slope stability of the upstream slope is calculated with the realized stresses with value of $F = 1.6$, i.e. it is greater than the required 1.5, for permanent load.

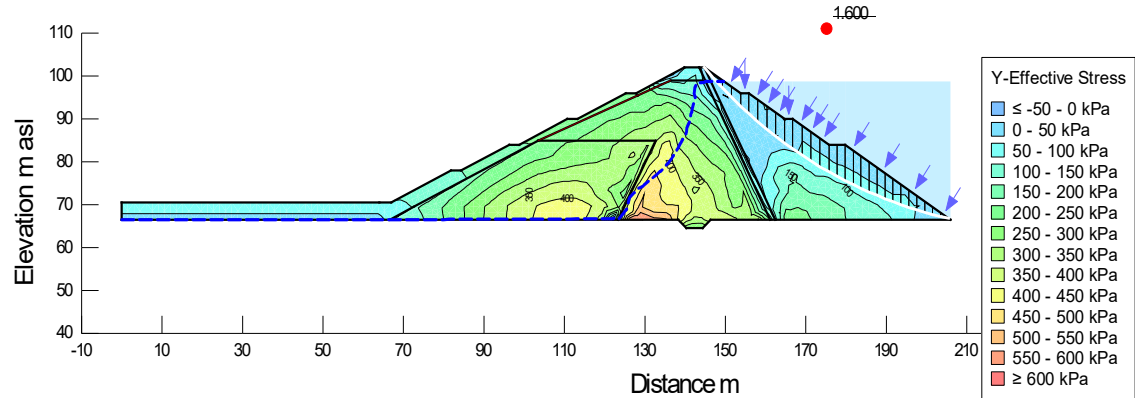


Figure 11. Initial state before earthquake action, distribution of vertical effective stresses, with coefficient of slope stability of the upstream slope $F = 1.6$.

3 DYNAMIC RESPONSE OF THE DAM

3.1 *Dynamic material parameters and model for permanent displacements*

In the dynamic analysis, a nonlinear model with variable maximum shear modulus is applied for the materials in the dam body, Figure 12. Dynamic analysis is performed with equivalent linear analysis (ELA) with inelastic dynamic parameters of local materials, Figures 13 and 14.

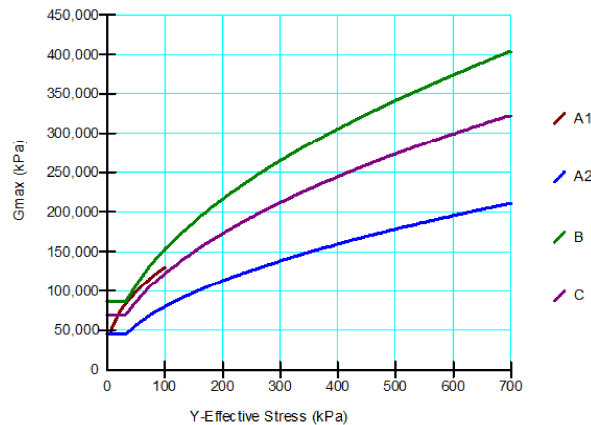


Figure 12. Variable maximum shear modulus $G_{\max} = G(\sigma_y')$ for local materials in the dam body.

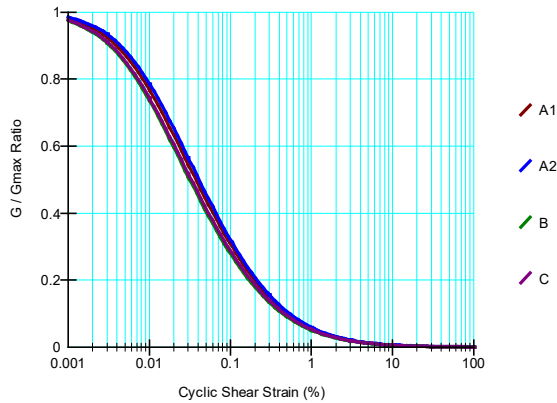


Figure 13. Reduction of the shear modulus with increase of tangential strains for local materials using an equivalent linear model.

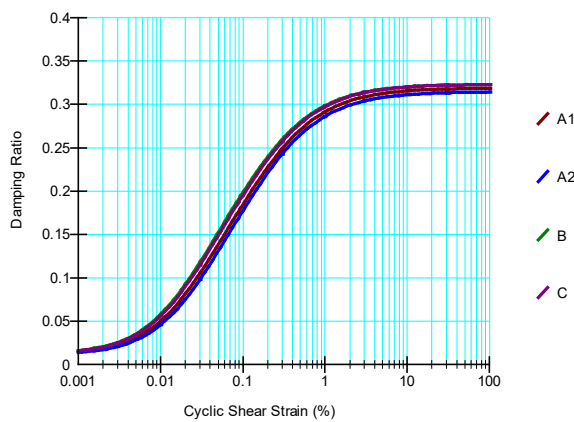


Figure 14. Increase in damping coefficient with increase in tangential strains for local materials using an equivalent linear model.

The approach applied in the present analysis for determination of the permanent deformations during the seismic excitation, for any node within the fill dam, is the method of "Dynamic Deformation Analysis" (DDA), which is successive non-linear redistribution of the stresses [2]. By such method, for geo-medium discretized by finite elements, are calculated deformations caused by forces in nodes, calculated by the incremental stresses in the elements. Thus, by application of non-linear model, for each time step of the dynamic response of the structure [6] is obtained new state of the total stresses and pore pressure. By the differences of the effective stresses in two successive time steps are obtained incremental forces, resulting in deformations, in accordance with the chosen constitutive law for dependence stress - strain. So, for each loading case during the dam's dynamic response are produced elastic and eventual plastic strains. If dynamic inertial forces cause plastic strains, then in the geo-medium will occur permanent deformations. The permanent displacements, at any point in the dam and at the end of the seismic excitation, are cumulative sum of the plastic deformations.

3.2 *Eigen periods of the dam*

To determine the eigen periods for a certain level of inelastic response of the embankment dam, a dynamic excitation of synthetic harmonic vibration with continuous change of frequencies was used, i.e. with evenly represented frequencies in the interval $f_1 \div f_2 = 0.4 \div 10.0$ [Hz] = $2.5 \div 0.1$ [s]. This harmonic has a maximum amplitude $A_0 = 0.001$ g, a total duration $S_t = 12$ [s], a time increment in the accelerometer $dt = 0.01$ [s], Figure 15. Spectra of excitation response and response, spectral acceleration S_a [g] for damping coefficient $DR = 0.05$, is given in Figure 16 for full reservoir. The dynamic response of the dam is determined using the Quake / W program [3].

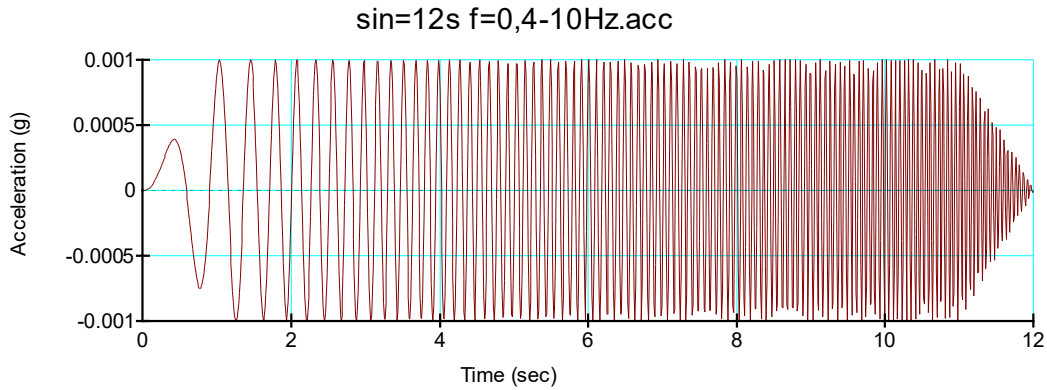


Figure 15. Time history of horizontal accelerations of harmonic vibration with evenly represented frequencies $f_1 \div f_2 = 0.4 \div 10.0$ [Hz], scaled with $A_o = 0.001$ g.

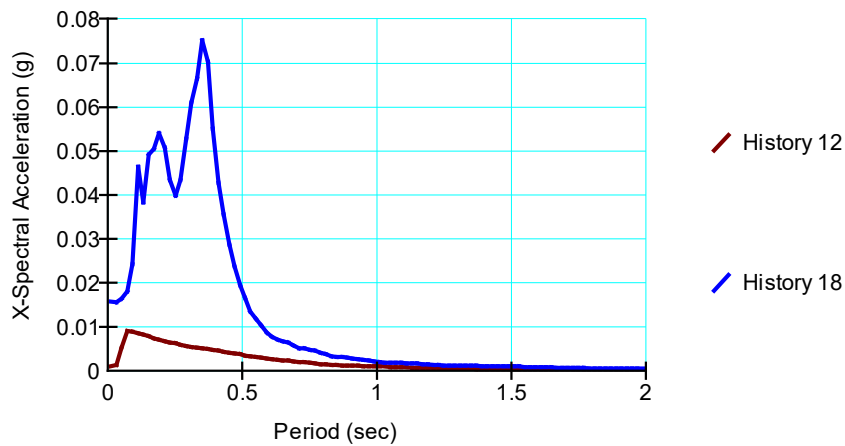


Figure 16. Response spectrum of absolute accelerations in the crest of the dam at full reservoir, caused by harmonic oscillation with low intensity $PGA=0.001$ g, with eigen periods $T_1=0.35$ s, $T_2=0.19$ s, $T_3=0.11$ s.

3.3 Seismology parameters of a strong earthquake

As a basis for generating accelerogram for synthetic earthquake, design spectra are adopted - spectra of elastic response to normalized accelerations from design earthquakes. In the analysis, the design spectra according to the Eurocodes (Eurocode 8, 2003) were used, for type A base for horizontal and type 1 for vertical component. Accelerogram of the horizontal and vertical components of a strong earthquake are given in Figures 17 and 18.

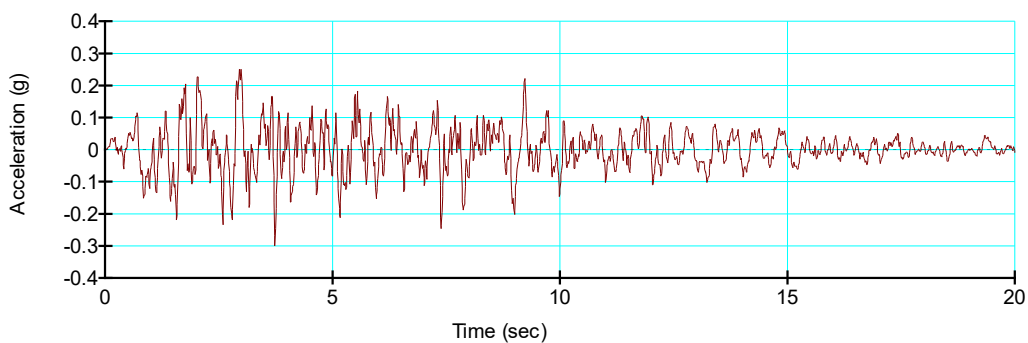


Figure 17. Time history of the horizontal excitation component in the rock foundation for a strong earthquake, $PGA_x = 0.3$ g.

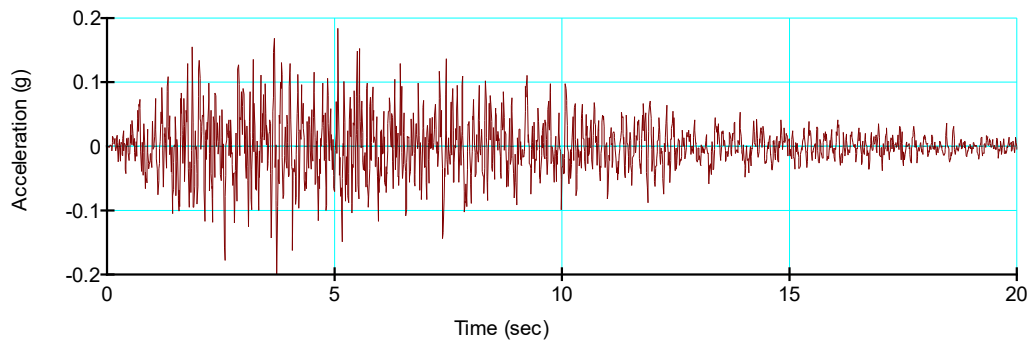


Figure 18. Time history of the vertical excitation component in a rock foundation for a strong earthquake, $PGA_y = 0.2 \text{ g}$.

3.4 Dam response during a strong earthquake

The horizontal accelerations in the dam crest at occurrence of a strong earthquake are given in Figure 19, and the response spectrum of the accelerations is given in Figure 20.

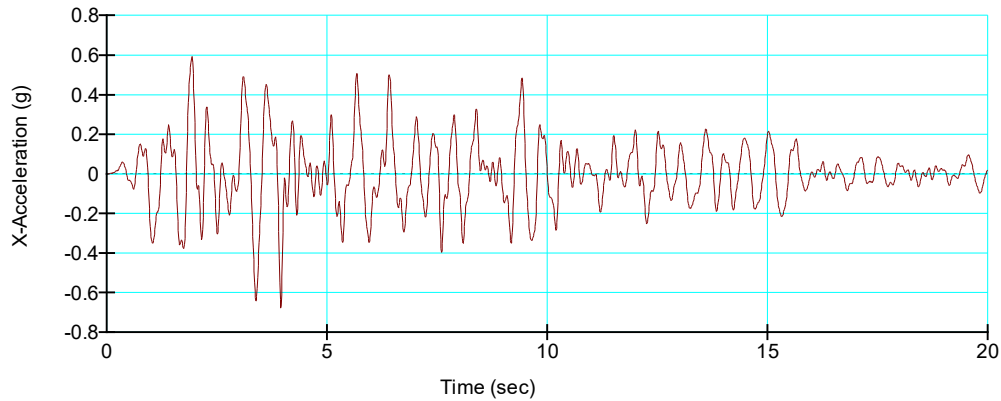


Figure 19. Time history of the horizontal component of the response in the crest of the dam with $PCE = 0.671 \text{ g}$, under the action of a strong earthquake with $PGA = 0.3 \text{ g}$.

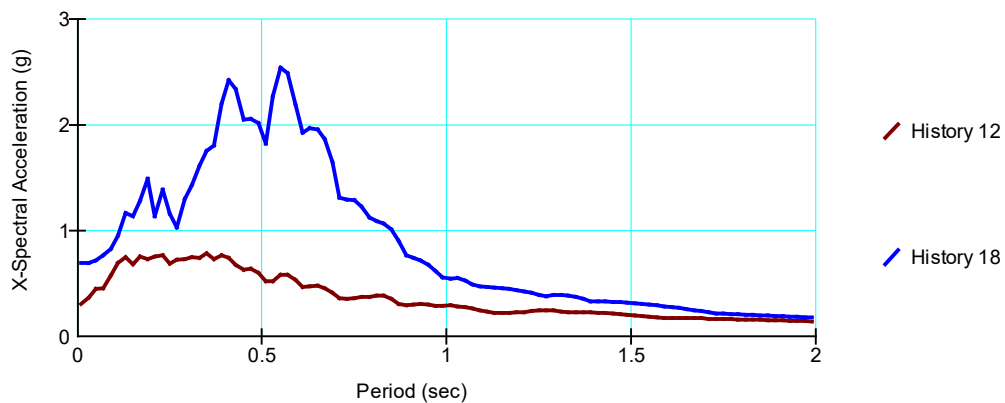


Figure 20. Response spectrum for the accelerations in the base and in the crest of the dam (with $T_1 = 0.55 \text{ s}$) during the action of a strong earthquake.

The relative displacements in the crest of the dam during the action of this earthquake are given in Figure 21.

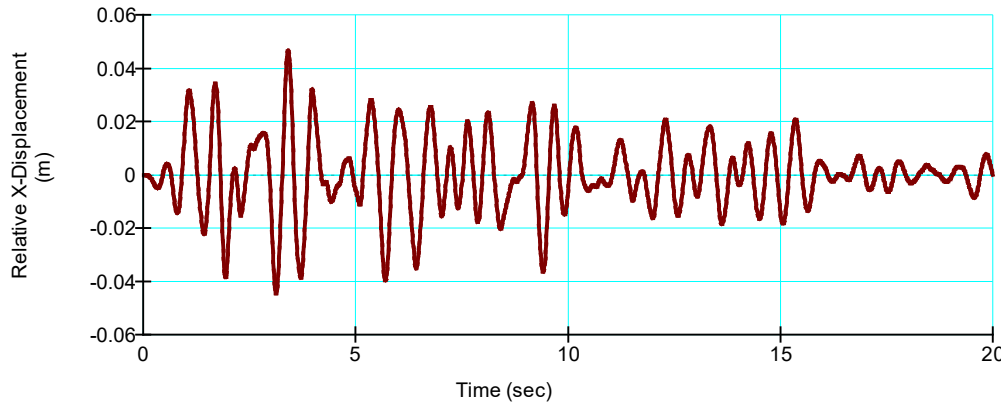


Figure 21. Time history of relative horizontal displacements in the dam crest during a strong earthquake.

The realization of the permanent horizontal and vertical displacements in the crest of the dam during the action of this earthquake are given in Figures 22 and 23, and after the action of the earthquake the permanent XY displacements in the body of the dam are given in Figure 24.

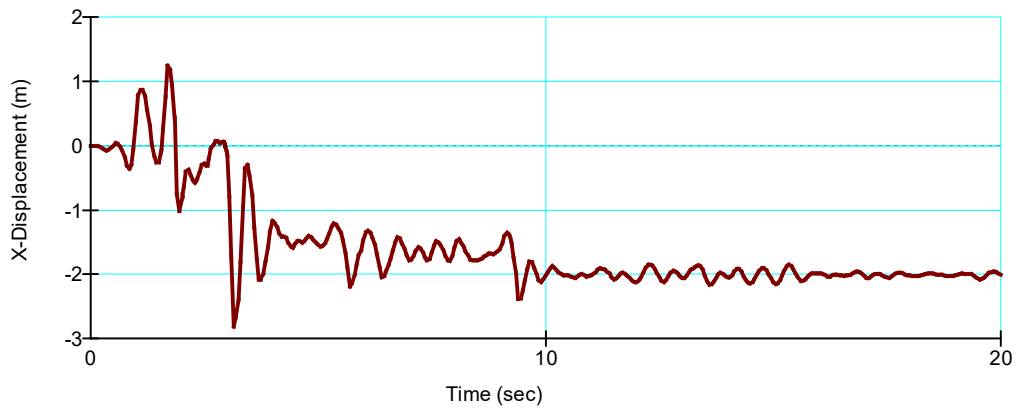


Figure 22. Permanent horizontal displacements in the dam crest (measuring point V5) during a strong earthquake.

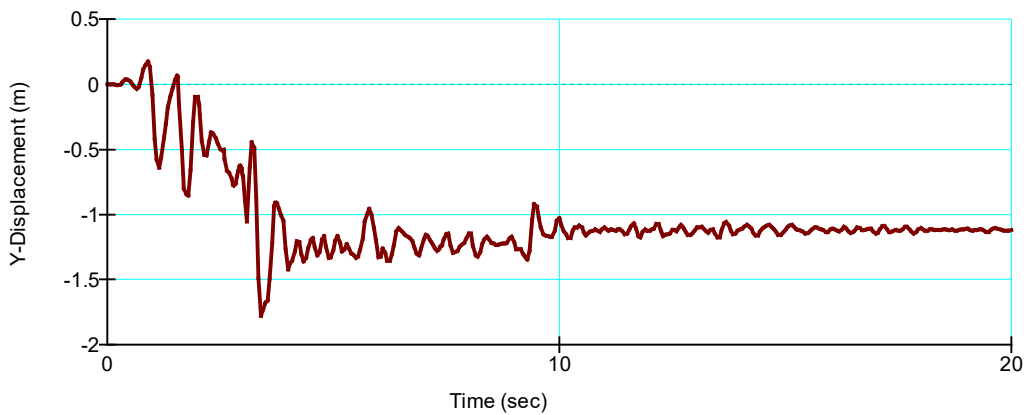


Figure 23. Permanent vertical displacements in the dam crest (measuring point V5) during a strong earthquake.

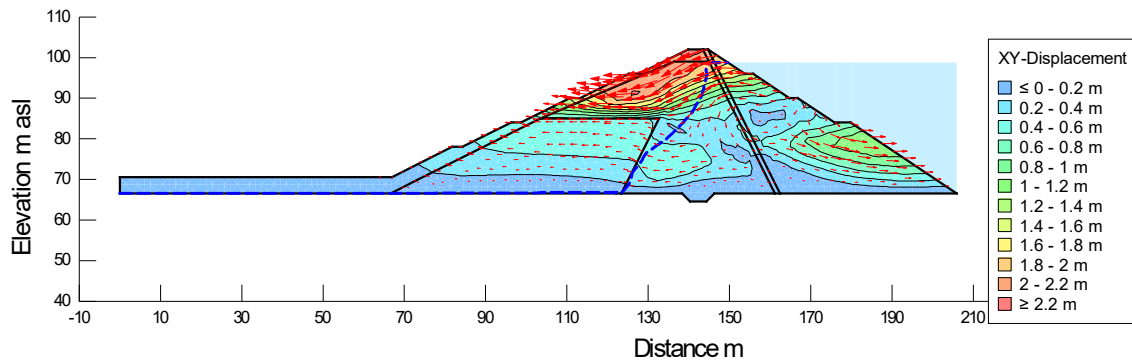


Figure 24. Permanent XY displacements in the dam after the action of a strong earthquake, $XY_{max}=2.3$ m.

4 CONCLUSION

The behavior of the dam during the filling of the reservoir, during the variation of the levels in the reservoir in the service period, and during the seismic excitation is simulated with only one model for structural analysis [6]. This ensures the transfer of the stress state in the analysis, as the initial state for each subsequent load case. The analyzes were performed using the effective stresses, i.e. by simulating of the increase and dissipation of the pore pressure in the drained conditions, with a coupled mechanical and hydraulic response with non-steady seepage.

In the static analysis, for the local materials in the body of the dam, an elastoplastic model with variable modulus of elasticity is applied, with calibrated elastic parameters. Criterion for calibration is the horizontal displacements in the crest of the dam, for the condition of the first filling of the reservoir, to be approximately the same with the measured values, i.e. about -120 mm in the downstream direction.

By extrapolating the displacements in the crest by 2027, under the proper behavior of the dam, a horizontal downstream displacement of 300 mm and a settlement of approximately 300 mm can be treated.

The stability of the dam is analyzed through the coefficient of slope stability (F) with the realized stresses, determined by the FEM model. The determination of coefficient F is performed only for the upstream slope, because with the adopted geometry and layout of the materials, it is obvious that the downstream slope has $F > 2$ for any load case. For the initial condition before the first filling is obtained $F = 1.33 > 1.3$, required for temporary load. For the state of full reservoir is obtained $F = 1.6 > 1.5$, required for permanent load. For the condition of rapid drawdown of the level to remediation elevation (82.0 m.a.s.l.), by applying the Limit Equilibrium Method, a safety coefficient $K_c = 1.373 > 1.3$, required for temporary load, is obtained. For this state, we emphasize that due to the high normal stresses (generated by the hydrostatic load during filling), the safety coefficient F calculated with the realized stresses is extremely higher. The key conclusion from the static analysis is that the embankment dam, with the adopted geometry and composition of the materials, possesses satisfactory static stability.

The dam's Eigen Periods are determined by the response spectrum when it is excited by harmonic vibration, with equal frequencies from 0.4 to 10.0 Hz, for the initial stress state at full reservoir. For low excitation intensity with $PGA = 0.001$ g, eigen periods $T_1 = 0.35$ s, $T_2 = 0.19$ s, $T_3 = 0.11$ s are obtained. For higher excitation in a strong earthquake with $PGA = 0.3$ g the response of the embankment dam is nonlinear, the stiffness of the local materials decreases with the increased inelastic deformations, which causes an increase of the period of the eigen tone $T_1 = 0.55$ s [7]. The values for the base tone (T_1), determined in the analysis, match the measured values for dams exposed to strong earthquakes in Japan [8,9], which is the best confirmation of the correctness of the adopted dynamic material parameters for nonlinear dynamic analysis.

The values for Dynamic Amplification Factor, where $DAF = PCA / PGA$, where PGA - Peak Ground Acceleration (in the horizontal direction), and PCA e Peak Crest Acceleration in the horizontal direction) are: $0.671 / 0.3 = 2.24$ for a strong earthquake. The response in the crest of the dam corresponds to the registered data on the degree of dynamic amplification of this type of

structures under the action of strong earthquakes, [10] and the time history of relative displacements are the key indicator for the correctness of the dynamic analysis.

The permanent settlements in the dam crest, caused by the dynamic inertial forces for the duration of the earthquake, determined by the method of Dynamic Deformation Analysis (DDA), is $Y = -1.1$ m for a strong earthquake. Regardless of the fact that the subject analysis does not take into account the settlements from additional compaction and reduced stiffness of materials exposed to cyclic action, the total settlement cannot exceed the height of the dam crest (102 m.a.s.l.) to the normal level in the reservoir (98.8 m.a.s.l.).

The key conclusion from the dynamic analysis is that the embankment dam, with the adopted geometry and layout of the materials, has satisfactory seismic resistance. That is, there is no violation of the water resistance of the waterproof body (wide clay core), nor is there a danger of rapid and uncontrolled emptying of artificial lake, because the settlement during the design earthquake with PGA 0.3 g does not overcome the protective height of 3.2 m.

REFERENCES

- [1] Zhvanut P., ..., (2022). 16th International Benchmark Workshop on Numerical Analysis of Dams, Theme C, Ljubljana, Slovenia
- [2] Geo-Slope SEEP/W v8, (2017). "Seepage analysis", GEO-SLOPE International Ltd., Calgary, Alberta, Canada.
- [3] Geo-Slope SIGMA/W v8, (2017). "Stress/deformation analysis", GEO-SLOPE International Ltd., Calgary, Alberta, Canada.
- [4] Geo-Slope SLOPE/W v8, (2017). "Stability analysis", GEO-SLOPE International Ltd., Calgary, Alberta, Canada.
- [5] Geo-Slope QUAKE/W v8, (2017). "Dynamic Modeling", GEO-SLOPE International Ltd., Calgary, Alberta, Canada.
- [6] Petkovski L., Tančev L., Mitovski S., (2007) "A CONTRIBUTION TO THE STANDARDISATION OF THE MODERN APPROACH TO ASSESSMENT OF STRUCTURAL SAFETY OF EMBANKMENT DAMS", 75th ICOLD Annual Meeting International Symposium "Dam Safety Management, Role of State, Private Companies and Public in Designing, Constructing and Operation of Large Dams", 24-29 June 2007, St.Petersbourg, Russia, Abstracts Proceedings p.66, CD-ROM
- [7] Park D.S., (2018). Fundamental Period of Embankment Dams Based on Strong Motion Records, Topic Earthquakes - Embankments, USSD 38th Annual Meeting and Conference, A balancing Act: Dams, Levees and Ecosystems, April 3- May 4, 2018, Miami, Florida, USA, CD Proceedings
- [8] Matsumoto N., ..., (2005). "ANALYSIS OF STRONG MOTIONS RECORDED AT DAMS DURING EARTHQUAKES", 73rd Annual Meeting of ICOLD, Tehran, IRAN, Paper No.: 094-W.
- [9] Fry J.J., Matsumoto N., (2018). Validation of Dynamic Analyses of Dams and Their Equipment, CRC Press/Balkema, Taylor & Francis Group, London, New York, ISBN: 978-0-429-49116-0 (eBook)
- [10] ICOLD, Bulletin 113, (1999). Seismic observation of dams - Guidelines and case studies